SPECTRAL DEPTH ESTIMATION AND UPWARD CONTINUATION ANALYSIS OF PARTS OF BORNO BASIN, NIGERIA USING AEROMAGNETIC DATA

In this study, spectral depth and upward continuation analysis of the residual magnetic field values covering parts of Borno Basin have been used to study the subsurface structure in parts of Borno Basin with a view to determining the hydrocarbon of the area. The study area extends from the latitude $12^{o}\,00'$ to $13^{o}\,50'$ North and longitude $12^{o}\,00'$ to $13^{o}\,50'$ East and is covered by eight (8) aeromagnetic maps. The maps were digitized on a 19 by 19 grid layout and recorded on coding sheets which were merged to generate a composite dataset and of which a composite map of the area was produced. The Polynomial method of filtering was applied to obtain a regional-residual separation. The filtered residual map was Fourier transformed after dividing the whole area into sixteen (16) overlapping blocks. The resultant logarithm of spectral energy and frequency were plotted graphically and the depths to the magnetic source were estimated. The first layer depth varies in thickness from 0.18 km minimum to 0.37 km maximum. The second layer (h_2) depth varies from a thickness of 1.79 km minimum to 5.34 km maximum. The first magnetic layer is attributed to lateritic ironstone, ferruginous sandstone and effect of surrounding basement rocks while the second layer is attributed to magnetic rocks intruded onto the basement surface, lateral discontinuities in basement susceptibilities and inter-basement features like faults and fractures. The second layer thus represents the depth to basement in the area and this depth has a maximum thickness of 5.34 km. The second layer (h_2) depth contour map and 10 km upward continuation map of the total magnetic intensity of the study area show that the northeast between latitude

CHAPTER ONE

1.0 INTRODUCTION

1.1 The Field of Applied Geophysics

The science of geophysics applies the principles of physics to the study of the Earth. Geophysical investigations of the interior of the Earth involve taking measurements at or near the Earth's surface that are influenced by the internal distribution of physical properties. Analysis of these measurements can reveal how the physical properties of the Earth's interior vary vertically and laterally (Kearey, Brooks and Hill, 2002). The cardinal point in applied geophysics is to add a third dimension to geological maps. The trained eye of the field geologist is replaced with the scientific instrument whose function is to detect changes in the physical properties of the rocks which lie concealed beneath the surface of the earth. Thus, geophysics involves the study of those parts of the earth hidden from direct view by measuring their physical properties with appropriate instrument, usually on the surface. It also includes interpretation of the measurements to obtain useful information on the structure and composition of the concealed zones (Telford, Geldart, Sheriff and Keys, 1976).

The initial step in the application of geophysics to the search for minerals probably was taken in 1843 when Von Wrede pointed out that the magnetic theodolite used by Lamont to measure variations in the earth's magnetic field, might also be employed to discover magnetic ore bodies (Telford *et al*., 1976). The continued expansion in the demand for metals of all kinds and the enormous increase in the use of oil and natural gas during the past fifty years have led to the development of many geophysical techniques of ever-increasing sensitivity for the detection and mapping of unseen deposits and structures (Telford *et al*., 1976). Advances have been especially rapid during the past two decades or so because of the development of new electronic devices for

field equipment and the wide spread application of the digital computer in the interpretation of geophysical data (Telford *et al*., 1976).

Since the great majority of mineral deposits are beneath the surface, their detection depends upon those characteristics which differentiate them from the surrounding media. Methods based upon variations in the elastic properties of rocks have been developed for determining structures associated with oil and gas, such as faults, anticlines and synclines, though these are often thousands of metres below the surface. The variations in the electrical conductivity and natural currents in the earth, the rates of decay in the artificial potential differences introduced into the ground, local changes in gravity, magnetism and radioactivity - all provide information to the geophysicist about the nature of the structures below the surface, thus permitting him to determine the most favourable places for locating the mineral deposits he seeks.

Geophysical Survey is the systematic collection of geophysical data for spatial studies. It may use a great variety of sensing instruments, and data may be collected from above or below the earth's surface or from aerial or marine platforms. Geophysical surveys have many applications in Earth science, archaeology, mineral and energy exploitation and engineering. Geophysical surveys are used in industry as well as for academic research. There are many methods and types of instrumentation used in Geophysical surveys. Technologies used for geophysical surveys include:

i. Seismic methods such as reflection seismology, seismic, refraction and seismic tomography.
ii. Magnetotellurics
iii. Transient electromagnetic (EM)
iv. Radio Frequency electromagnetic propagating (e.g. ground penetrating radar)

v. Electrical techniques including electrical resistivity, induced polarization and spontaneous potential.

vi. Magnetic techniques include aeromagnetic surveys and magnetometer.

vii. Gravity and gravity gradiometer

viii. Geodesy

ix. Remote Sensing

x. Seismo-electrical method

Geophysics techniques can therefore only detect a discontinuity, that is, where one region differs sufficiently from another in some property. Applied geophysics in the search for minerals, oil and gas may be divided into the following general methods of exploration: gravity, magnetic, electrical, electromagnetic, seismic, radioactivity, well logging and miscellaneous chemical, thermal and other methods. The choice of technique or techniques to locate a certain mineral depends upon the nature of the mineral and the surrounding rocks (Telford *et al*., 1976).

1.2 The Aeromagnetic Survey

The study of the earth's magnetism is the oldest branch of the subject of geophysics. Sir William Gilbert (1540-1603) made the first scientific investigation of the terrestrial magnetism when he showed that the earth's magnetic field was equivalent to that of a permanent magnet, lying in a general north-south direction, near the earth's rotational axis (Telford *et al*., 1976). In 1843, Von Wrede first used variations in the magnetic field to locate deposits of magnetic ore. The publication of the Examination of Iron Ore Deposits by Magnetic Measurements by Thalen in 1879 marked the beginning of applied geophysics (Telford *et al*., 1976).

The cardinal point of a magnetic survey is to find the distribution of magnetized material whose magnetic field is given on a plane surface. Magnetic prospecting thus involves the measurement of variations in the earth's magnetic field (Kearey *et al*., 2002). It is natural source methods in which local variations introduced by magnetic properties of rock near the surface causes minute changes in the main field. Determination of the structure and nature of the magnetized material is therefore an inverse problem of potential field theory. That is, the source is determined from its potential (Grant and West, 1965). Magnetic exploration is carried out on land, at sea and air. Until the middle 1940s, all magnetic exploration was carried out on the ground using field methods similar to those in gravity surveys. Today, virtually all magnetic survey for oil is done from the air or ships. This is also true for most reconnaissance surveys for minerals (Kearey *et al*., 2002). The speed, economy and convenience of aeromagnetic surveys are the main factors for this trend.

Aeromagnetic interpretation is the drawing of inferences about the geology and ore potential of a given region from aeromagnetic survey data. The major magnetic minerals are magnetite, titanhematite, maghemite, pyrotite, and native iron ore Fe-Ni-Co alloys. These minerals give rise to magnetic anomalies, either because of their abnormally large magnetic susceptibilities or because they have high remanent magnetization. Of the magnetic minerals that occur in nature, magnetite is the most abundant. On a global basis, the others can probably be ignored (Grant, 1978). Thus aeromagnetic surveys, in particular terms, map the magnetite in the rocks below the aircraft. While aeromagnetic surveys are extensively used as reconnaissance tools, there has been an increasing recognition of their value for evaluating prospective areas by virtue of the unique information they provide (Kearey *et al*., 2002).

The roles of aeromagnetic survey are as follows:

i. Delineation of volcano-sedimentary belts under sand or other recent cover, or in strongly metamorphosed terrains when recent lithologies are otherwise unrecognizable.

ii. Recognition and interpretation of faulting, shearing and fracturing not only as potential hosts for a variety of minerals, but also an indirect guide to epigenetic, stress related mineralization in the surrounding rocks.

iii. Identification and delineation of post-tectonic intrusive. Typical of such targets are zoned syenite or carbonatite complexes, kinerlites, tin-bearing granites and mafic intrusions.

iv. Direct detection of deposits of certain iron ores.

In prospecting for oil, aeromagnetic data can give information from which one can determine depths to basement rocks and thus locate and define the extent of sedimentary basins. Sedimentary rocks however exert such a small magnetic effect compared with igneous rocks that virtually all variations in magnetic intensity measurable at the surface result from topographic or lithologic changes associated with the basement or from igneous intrusions (Dobrin, 1976).

1.3 Location of the Study Area

The study area covers parts of the Borno Basin from latitude $12^{o}\,00'$ to $13^{o}50'$ North and longitude $12^{o}00'$ to $13^{o}50'$ East, which makes up of a square block 24 200 km^2. The Schist belt (Kerikeri formation) and the younger granites region of the Jos and Bauchi areas are found in the area, which is situated at the northeastern part of Nigeria as shown in Figure 1.1. The physiological features recognized in the area are the river Benue and its tributaries like river Gongola, Amumma, Rowai, Ruhu, Misau and so on. Also, the magnetic lineaments interpreted by Ajakaiye *et al.* (1991) as St.

Paul, Romanche and Chain ancient fractured zones were noticed as lineaments passing through the study area.

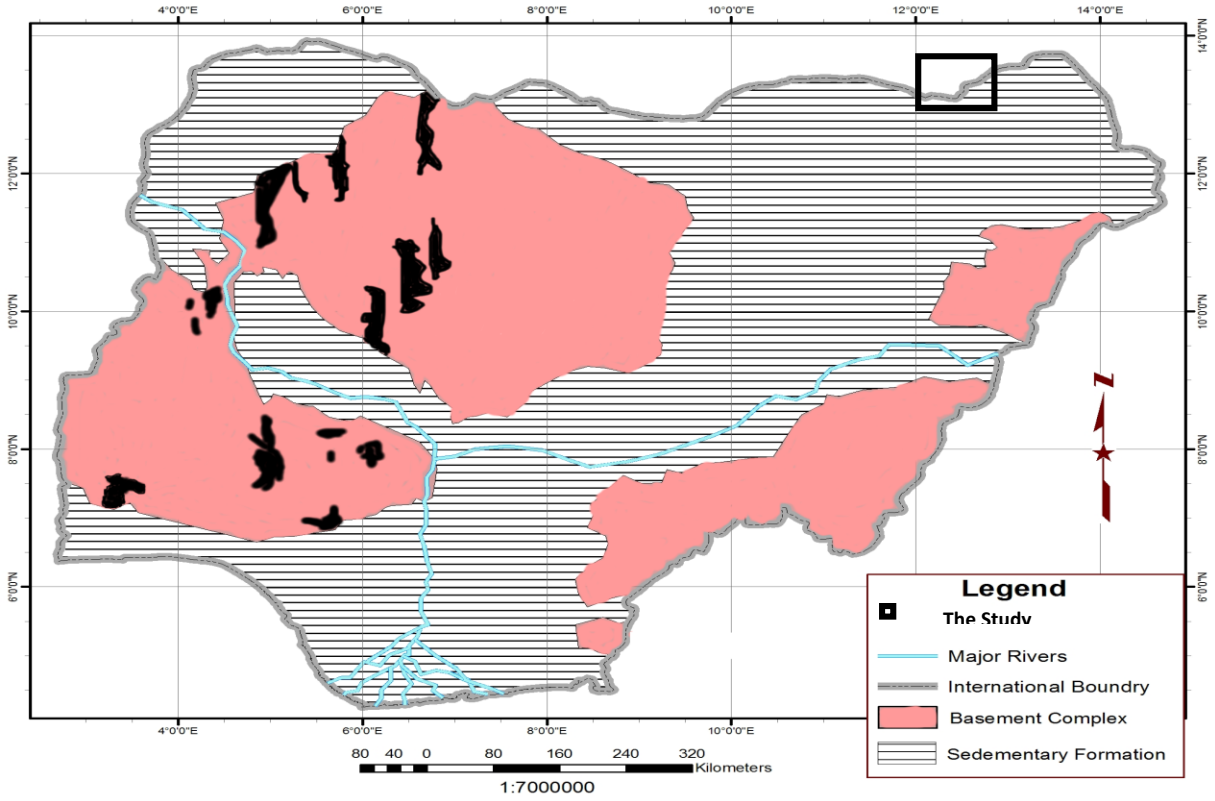

Figure 1.1: General geology Map of Nigeria Showing the Sedimentary Formation Location of the Study Area

1.4 Statement of the Problem

The majority of mineral deposits are beneath the earth surface. The overdependence on hydrocarbons in the Niger Delta part of Nigeria may lead to overstretching of the area and eventually the complete phase out of these deposits.

This research is focusing on finding the most favourable place for locating the mineral deposits in Borno basin through quantitative and qualitative interpretation of both spectral depth estimation and upward continuation analysis. This new source of hydrocarbon will serve as supplement to the existing sources of hydrocarbons in Nigeria.

1.5 Justification of Study

The use of digital processing tools on the aeromagnetic data of the study area is expected to shed more light on the historical evolution and tectonic setting of the study area (the parts of the Borno Basin and their surrounding basement rocks). This would be justified as very little is known concerning interpreted magnetic signatures over the Borno Basin. These digital tools would be combined in such a manner to investigate and interpret the aeromagnetic data covering the study area and thus the emerging picture is expected to give more information on the basin.

1.6 Aim and Objectives

The aim of this study is to determine the estimated depths to magnetic ensembles in parts of Borno basin using aeromagnetic data.

The following are the outlines of the objectives of the study:

i. To estimate the thickness of structure at the subsurface of parts of Borno Basin.
ii. To determine the economic potentials of the study area in terms of hydrocarbon and mineral resource potentials.

iii. To carry out a surface mapping of the total aeromagnetic data of the study area and qualitatively analyze the trend so as to determine prominent structural trend within the area.

iv. To perform upward continuation of the total intensity magnetic data to enhance location of prominent anomalies with the study area.

v. Delineation of the magnetic mineralization of the study area.

CHAPTER TWO

2.0 LITERATURE REVIEW

2.1 Geology of the Study Area

The study area covers parts of Borno Basin, and the Basement Complex as shown in Figure 2.1. All the rocks in the area belong either to the Upper Cretaceous or to the Precambrian. All the above mentioned units have already been described in detail by various workers (McCurry, 1976; Ajibade, 1976; Eborall, 1976; Wright, 1976). (The sandstones of the parts of the Borno Basin belong to the Upper Cretaceous and they are underlain by the Precambrian rocks of the Basement Complex).

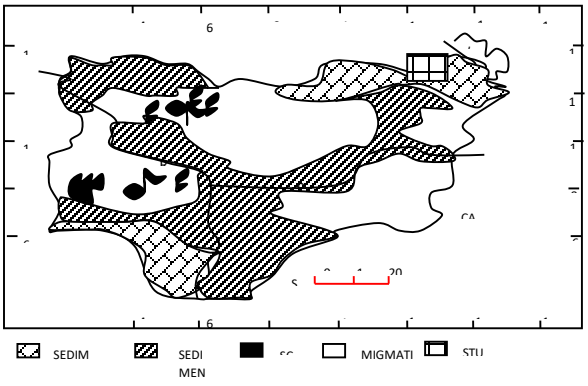

Figure 2.1: General Geology Map of Nigeria Showing the Location of the Study Area (Adapted from Geology map of Nigeria produced by the Geological Survey Agency of Nigeria, 2006)

2.2 General Geology of the Basement Complex

The Basement Complex is exposed over nearly half of Nigeria (Figure 1.1). It extends in the west into the Dahomeyan of the Benin Republic and in the east into the Cameroons. In the remaining half of the country Cretaceous and younger sediments cover the Basement Complex. The Nigeria Basement Complex is believed to be mostly Precambrian in age. However, it probably contains intrusions of Paleozoic age (Oyawoye, 1964). The earliest study of the Complex was made by Falconer (1911) who recognized the age distinction between the Precambrian Older Granites and the Jurassic "Younger" Granites of Jos Plateau. He also introduced these terms.

The geology of the Basement Complex is quite complicated. The terrain involved represents a level at considerable depth in the earth which has now been exposed through erosion over several million years (Oyawoye, 1964). The rocks have been involved in multiple folding, fracturing and igneous activities. The rocks of the Nigeria Basement Complex can be grouped into three litho logical units (Ajibade, 1980). These are:

(i) The migmatite-gneiss complex which covers about 70% of the whole Basement Complex

(ii) The metasediments and metavolcanics which form the schist's belts and

(iii) The Older Granites which intruded both the migmatite-gneiss complex and the schist's belts.

The migmatite-gneiss complex is the largest unit in the Basement Complex and consists essentially of migmatites, quartzo-feldsparthic-biotite-hornblend gneiss with relict metasedimentary rocks. Following the formation of the gneisses, a period of sedimentation intervened and predominantly fine-grained rocks were deposited, probably in moderately deep water. During the episode of compression which followed sedimentation, these beds were isoclinically folded and largely

converted to schists. The metasediments and metavolcanics form the schist's belts. Mapped outcrops of these are mainly found in western half of the country. They consist of low grade metamorphosed sedimentary rocks with associated volcanic rocks. Their age is believed to be between 1000 and 800 Myrs (McCurry, 1976). The metasediments are thought to have once covered the whole Basement Complex area. They have been removed by subsequent erosion and are now preserved in synclinal troughs (McCurry, 1976).

After the folding of the sediments and the formation of the metasediments and metavolcanics, there followed a period of granitic intrusion. This was the Older Granite cycle, known throughout Nigeria (Falconer, 1911; Russ, 1957; Trustwell and Copel 1963). The Older Granites are bodies of igneous rock of various compositions, ranging from true granites to tonalites and charnochitic rocks which intruded both the migmatite-gneiss complex and the schist's belts. They occur as elongated Batholiths or small circular plutons. Age determinations on the Older Granites all over Nigeria have yielded Pan-African age- 600yrs (Grant, 1978).

2.2.1 Geology of the Younger Granite of Jos and Bauchi Area

The origin and evolution of the Younger Granites has been a subject of controversy between those who favour a plume hypothesis and others who support lithospheric controls. For example, the magmatism responsible for the alkaline ring complexes has been related to either the action of mantle plumes beneath the lithosphere or to intraplate deformation with reactivation of deep fractures (Ajakaiye, Hall and Millar, 1985). Also, an inverse correlation between periods of alkaline magmatism the periods of rapid displacements of the African plate has been noted and has been interpreted as indicating that intraplate magmatism occurs where there is interference and collision along the African plate (Black *et al.,* 1979). In addition, alkaline ring complexes have

been interpreted as being related to rifting and to transform faults (Ajakaiye, 1970). They have also been found to align along directions corresponding to an early arc of rotation and are thought either to precede and predetermine the oceanic transform faults or to have occurred later during reactivation of fractures situated at the ends of the oceanic transform faults (Black *et al.*, 1979).

2.2.2 The Geology of the Cretaceous Sediments in the Northeast Nigeria

Nigeria contains some of the most extensively developed and best studied Cretaceous successions known from Africa. The Cretaceous sediments almost everywhere lie directly upon crystalline basement rocks which belong to the Pan-African mobile belts (McCurry, 1976; Ajibade *et al.*, 1989). Previous review of the Cretaceous system in Nigeria was provided by Reyment (1965) and Whiteman (1982). Entries for Nigeria in editions of the Lexique Stratigraphique International were compiled by the Geological Survey of Nigeria (1956). Geological maps of the country were prepared by the Geological Survey of Nigeria (1974) and, with explanatory notes, by Dessauvagie (1974, 1975).

The intracontinental Benue Trough was initiated during the Lower Cretaceous in relation with the Atlantic Ocean opening. The first stage of its evolution started in the Aptian, forming isolated basins with continental sedimentation. The most important of the Cretaceous sedimentary basins is the Benue Trough, an integral part of the "West and Central Africa Rift System" (WCARS) of Fairhead (1986) and subsequent authors (Guiraud *et al*., 1992; Genik, 1993; Keller *et al.*, 1995).

2.3 Geology of the Borno Basin

The Borno Basin (also called "Maiduguri Sub basin" (Avbovbo *et al.*, 1986) makes up the southwestern part of the Chad Basin as shown in Figure 2.1). The Cretaceous sediments in the Borno Basin are almost entirely concealed by the continental Pliocene to Pleistocene Chad

Formation (Carter *et al.,* 1963; Barber, 1965; Miller *et al.* 1968) which reaches a thickness of over 1500 m (Olugbemiro, 1997). Descriptions of the Borno Basin have been given by Raeburn and Jones (1934), Matheis (1976), Avbovbo *et al.* (1986), Okosun (1995) and Olugbemiro (1997). Those parts of the Chad Basin to the north and east were reviewed by Bellion (1989) with important subsequent accounts having been given by Genik (1992, 1993). The latter provided detailed descriptions of the concealed east Niger, Bongor, Doba, Dosco and Salamat rifts. The Southern part of the Borno Basin is covered by the Geological Survey of Nigeria 1:250 000 Series map sheets 25 (Potiskum). Raeburn and Jones (1934), Barber (1965) and Miller *et al.* (1968) produced the geological maps of parts of the area to the north.

The present terms "Gongola Basin", correspond to the "Chad Basin" of Carter *et al.* (1963). A series of N-S to NNE-SSW trending faults controls the trend of the Gongola Basin (Zaborski *et al.,* 1998). The thickest sedimentary successions occur in the western part of the Gongola Basin to which Campano-Maastrichtian and Cenozoic deposits are restricted. Over 5km of sediments occur in the "Dukku", "Ako" and "Bashar" sub-basins; thinner successions occur in the "Lau" and "Numan" sub-basins of the Yola arm (Benkhelil, 1988, 1989). The Yola arm extends eastwards into Cameroun where it is known as the Garoua Basin.

Similarly, Cratchley (in Avbovbo *et al.,* 1986) recognize an ovoid-shaped negative Bouguer gravity anomaly north of Maiduguri. Combining the gravity data with seismic refraction studies, Cratchley *et al.* (1984) identified a "Maiduguri Trough", thought to contain some 3000 m of Cretaceous and Quaternary sediments, running NNE from near Maiduguri and connecting with the Termit rift. A positive regional gravity anomaly of about 45 mgal amplitude was associated with the Maiduguri Trough, by comparison with the Benue Trough, this anomaly being interpreted in terms of crustal thinning. Seismic reflection data of Avbovbo *et al.* (1986) inferred a total thickness

of over 10 km of Cretaceous to Quaternary sediments in the "Maiduguri depression". The Chad Formation has been attributed to a thermal sag stage of basin development subsequent to rifting in the WCARS (Fairhead, 1986, 1988a and 1988b; Fairhead and Okereke, 1987, 1990). Sahagian (1993) and Hartley and Allen (1994) believed that uplift of its periphery, notably that of the Hoggar, Air, Tibesti and Darfur domes, was the most important control on Neogene-Recent sedimentation in the Chad basin.

2.3.1 Stratigraphy and Sedimentation

The stratigraphy of the Borno Basin has largely been interpreted by comparison with the Upper Benue Trough. The Cretaceous succession in the Upper Benue Trough comprises Early Cretaceous continental clastics, the Bima Group, and a dominantly marine Late Cretaceous succession. The former include the oldest sediments known in the Benue Trough, deposited during active rifting. During the Late Cretaceous, thermo-tectonic sag conditions prevailed and sedimentation was strongly influenced by transgressive-regressive events. The Upper Cretaceous may be divisible into discrete pre-Santonian and Campano-Maastrichtian parts, the latter deposited during a renewed phase of rifting.

Carter *et al.* (1963) referred the outcropping sediments in the south-west (previously described by Jones (1932) and Raeburn and Jones (1934) to the Gongila Formation, Fika Shales and Gombe Sandstones. At Damagum and Maiduguri, to the north, 100 m and 450 m respectively of beds belonging to the Fika Shales were identified in boreholes which bottomed within the unit. On the northern flank of the Dumbulwa-Bage high, the Cretaceous outcrops was subdivided into the Kanawa, Dumbulwa and Fika members of the Pindiga Formation. The Fika member contains Coniacian ammonities and to the east, where the Dumbulwa member wedges out, its basal part

includes calcareous sandstones with Coilopoceras. Dolerite sills intrude the Fika member. Obi (1995, 1998) described a Cretaceous succession about 50 m thick outcropping along the central southern margin of the Borno Basin, an area referred to as "Hawal Basin". The following units were identified:

i. a coarsening-upwards succession divisible into: an upper part comprising about 13 m of bioturbated, calcareous fine-grained sandstones and siltstone, gypsum-bearing clay shale with small bivalves and gastropods and fine to medium-grained, laminated or cross–bedded sandstone with Ophiomorpha, Thalassinoides and Skoilithos*;* and a lower part comprising 12 m of alternating fine to medium-grained sandstones' bioturbated siltstone and shale;
ii. 16 m gypsum-bearing blue-grey clay shale with intercalated limestones;
iii. about 4 m of medium to coarse-grained, calcacereous often nodular sandstones and sandy claystones; and
iv. at least 5 m of pebbly sandstones directly overlying the Precambrian basement.

Unit i was referred to the Bima Group, ii to the Yolde Formation and iii and iv to the Gongila Formation.

Knowledge of the subsurface Cretaceous stratigraphy of the Borno Basin derives from seismic and boreholes studies. Avbovbo *et al.,* (1986) identified seven "seismic sequences" in the Maiduguri depression interpreted as:

i. the Chad Formation;
ii. the Keri Keri Formation, lying uncomformably upon the older folded and faulted succession;
iii. the Gombe Sandstone;
iv. the Fika Shale;

v. the Gongila Formation;

vi. the upper Bima Group;

vii. a unit regarded as distinct from the Bima Group, divisible into 1b above, seismically transparent and believed to be made up of marine shales; and 1a below, an inferred fault scarp fan and fluvial facies.

Okosun (1995) and Olugbemiro (1997) provided direct lithological data from boreholes located to the north of Maiduguri. The Cretaceous sediments are directly overlain by the Chad Formation; Keri Keri Formation and Gombe Sandstone are absent. Three or four Cretaceous units were identified: marine grey or blue-black shale, occasionally gypsum-bearing, with thin limestone intercalations and black shale horizons, referred to the Fika Shale. Diorite sills occur in places. A lectostratotype 890 m thick was proposed for the unit in the Kanadi-1 well by Okosun (1995) Dating of the Cretaceous sediments is in precise. Okosun (1992) assigned an age within the range of Turonian to Santonian to ostracods recovered from beds referred to the Fika Shale.

Correlation of the Cretaceous successions in the Borno Basin and Upper Benue Trough remains inexact. Okosun (1995) and Olugbemiro (1997) respectively suggested Albian to Turonian and Albian to Cenomanian ages for beds referred to the Bima Group in the Borno Basin. Lower Turonian and Turonian ages for the Gongila Formation; and Turonian to Maastrichtian and Turonian to Santonian ages for the Fika Shale. Okosun (1995) indicated the Kanadi well as bottoming in basement rocks, Olugbemiro reported only the Kinasar well as penetrating the full thickness of the Bima Group and “pre-Bima” beds. A notable feature of the succession in the later well in contrast to the Upper Benue Trough is relatively greater importance of the Upper Cretaceous marine beds compared to the equivalents of the Bima Group. Olugbemiro reported Heterohelix from the upper part of the Bima Group in the Mbeji well and arenaccous foraminifers

were recovered from “Bima” deposits in this, the Kanadi and Albarka wells. The earliest Cretaceous marine beds in the Upper Benue Trough and the Chad Basin to the north (Genik, 1993) are Cenomanian. It is unlikely that the “pre-Bima” shales of Avbovbo *et al.* (1986) are Albian marine deposits as these authors supposed. Olugbemiro suggested that sedimentation in the Borno Basin began only during the Albian to Cenomanian. This also conflicts with the Upper Benue Trough and Termit rift where sediments as old as latest Jurassic occur (Genik, 1993). Further data, including detailed dating of the Borno Basin sediments, is required to resolve these apparent discrepancies.

2.4 Economic Geology

The potential of the part of Borno Basin for resources of raw materials of economic significance is related to its form, origin and history as a rift which failed to develop into an ocean basin, and is compared to similar geological environments in other parts of the world. Deposits of limestone, brick and fire clay, construction stone, laterite and coal, some are being worked, while others are being investigated and new ones sought. Lignite is found with the highest rocks of the stratigraphic sequence at the seaward end of the trough, which could also be regarded as the earliest deposits of the present Niger Delta. Significant occurrences of base metal sulphides (lead and zinc, with smaller amounts of copper) cadmium and silver, and the associated minerals barites and fluorspar, and known to occur locally in spatial, and probably genetic, relation to salt water springs. The possibility of finding larger lower grade deposits of base metals is encouraging. Sources of glass sand and mineral (juvenile) water could have been valuable in more populated and otherwise developed parts of the country. The potential for large economic deposits of rock-salt (halite) is considered to be very good but other evaporate deposits such as gypsum and anhydrite, which may also occur, are likely to be too deep for commercial exploitation. The possibilities for oil and

natural gas are also worth further investigation, as is the potential for radioactive minerals within the sediments. The indication for large reserves of ground (meteoric) water is doubtful, most of the sedimentary formations lacking the necessary porosity and permeability.

The rift structure is too senile to yield any presently usable geothermal energy although there has been some fairly recent (Quaternary) volcanic activity and there are many warm springs. Combustible gases in these springs are only of importance as a hazard to underground mining, while the presence of rare gases has yet to be checked, but is unlikely to be in productive quantities (Ford, 1981).

2.5 Reviews of Geophysical Literature

The study area covers parts of the Borno Basin, the Schist belt (Kerikeri formation) and the younger granites region of the Jos and Bauchi areas. This area is situated at the northeastern part of Nigeria as shown in Figure 1.1. The area is bounded by latitude 12^{o} 00' N to 13^{o}50' N and longitude 12^{o} 00' E to 13^{o}5' E. The Borno Basin and the Benue Trough constitute the major part of the present study, the entire Benue Trough is believed to have evolved as a result of the continental separation of Africa and South America (King, 1950) and is variously described as a rift system (Crachley *et al*., 1984 and Jones, 1965) an extensional graben system, a third failed arm or an aulcogen of a three-armed rift system related to the development of domes associated with hotspots. The Benue Trough and indeed middle and upper Benue Trough, is filled with thick (average thickness of about 5 km) with varied lithological units (Likkasson *et al*., 2005).

2.6 Previous Geophysical Work in the Area

In Nigeria, extensive geophysical investigations have been largely confined to sedimentary formations with proven natural resource potentials. The Niger Delta area of southern Nigeria has

witnessed extensive gravity, magnetic and in particular seismic surveys in connection with oil and gas by oil industries operating in Nigeria. The Chad Basin has also attracted some attention in the decade mainly for oil and ground water purposes. Comprehensive geophysical investigations have also been done in the Benue Trough.

However, there are limited numbers of geophysical work as compared with that of the geological work in the study area.

Cratchley *et al*. (1965) carried out the first gravity survey in the middle and upper Benue Trough. They showed that the Bouguer isogals are generally parallel or sub-parallel to the margins of the trough. Two fundamental features were identified: a positive regional anomaly, with an amplitude of approximately 50 mGal and a mean width in excess of 150 km, interpreted as indicating a thinner crust below the basin compared to the flanking basement; and shorter-wavelength residual anomalies, comprising an axial positive anomaly flanked either side by negative anomalies, interpreted as representing an axial zone of shallow basement rocks containing basic to intermediate intrusive flanked by zones where the sedimentary infill reaches thicknesses of up to 6 km. subsequent estimates of the amount of crustal thinning below the Benue Trough have varied from as little as 1.5 km (Adighije, 1979, 1981) to over 10 km, according to the density contrast between the crust and upper mantle that was assumed (Ajakaiye, 1981). The short-wavelength axial gravity high has been interpreted as representing a dense intrusive "mantle diaper" (Adighije, 1979, 1981) or a zone of shallow basement rocks intruded to a greater or lesser extent by basic to intermediate magnetic bodies (Ajayi *et al*., 1981).

Stuart *et al*. (1985) carried out seismic refraction studies. His studies indicated that a crustal thickness of 23 km below the Garoua Basin (Eastern Yola arm) compared to a normal thickness

of 34 km to the south, and a density contrast between the crust and anomalously low-density mantle of 0.17 g cm^{-3}.

Ajakaiye *et al.* (1986) revealed the interpretation of aeromagnetic anomalies and tectonic trends in and around the Benue Trough, Nigeria shows that magnetic lineaments with definite characteristics exist within the Nigerian continental landmass. The study shows that the Benue Trough is part of a large-scale continental feature of global importance because its boundary faults can be linked to the chain and char cat feature zones in the mid-Atlantic.

Avbovbo *et al*. (1986) inferred a total thickness of over 10 km of Cretaceous to Quaternary sediments in the "Maiduguri depression" (less than 5 km was subsequently proved) from their seismic reflection data. Two main fault systems were identified, a dominant NE-SW trending and a subsidiary NW-SE trending set. The former involve the Precambrian basement, high-angle normal faults delimiting horst and graben-like features. The latter affects only the sediments. Nearly all the faults terminate at an angular unconformity separating Cretaceous from younger beds.

Ananaba *et al*. (1987) had on the basis of lineament of LANDSAT images identified predominate tectonic trends in the NE-SW, NW-SE and N-S directions over the Borno basin and in particular other parts of the country rejuvenated during the tectonic phase of the pan African oregeny.

Fairhead *et al*. (1987) carried out a new gravity data to investigate the nature and cause of the Bouguer gravity field associated with the Cretaceous West Africa rift system in Nigeria and Cameroon. The new gravity measurements included data collected over the basement area between the Benue Trough and the Cameroon border and fill an important gap in the gravity coverage.

Fairhead *et al*. (1988) estimated the depth to major density contrasts within the lithosphere over the West African Rift System and adjacent basement areas in Nigeria and Cameroon, based on the spectral analysis of the Bouguer gravity field. The study reveals that three main density discontinuities occur in the depth ranges 7 to 12 km, 19 to 30 km and 80 to 93 km.

Fairhead *et al*. (1989) carried out a gravity modeling to determine the African rifting system and tectonic model for Nigeria and East Niger rift basins. They discovered that since early Mesozoic times, three phases of rifting have occurred in Africa and are related to distinct phases of breakup of Gondwana. These contrasting rift episodes have provided an insight to the extent to which plate tectonic processes and more localized mechanical anisotropy processes within the Africa lithosphere have influenced rifting. Gravity modeling of the Nigeria and East Niger rift basins shows the extent and nature of the broad (regional) positive Bouguer anomaly associated with these rifts. The removal of this regional anomaly allows the delineation of the (residual) negative Bouguer anomaly which reflects the lateral extent and thickness of Msozoic and Cenozoic sediments.

Guiraud *et al*. (1991) revealed that the northern section of the Cretaceous Benue Trough in Nigeria presents several major faults zones striking N 30^{o} E to N 60^{o} E cross-cutting both sedimentary and Precambrian basement rocks in the area. The Mesozoic deposits in the area are also deformed by the NE-SW to N 80^{o} E trending asymmetric large scale folds (Lamurde and Jarawa anticlines, Dadiya syncline). A detailed micro-tectonic study of the deformed tectonic zones has been carried out, mainly along the major faults zones (Gombe, Burashika, Kaltungo and Teli areas) on the sedimentary basin and on the Pan-Africa basement (Plateau and Gurukusa areas) surrounding the basin. At each micro-tectonic station, a significant population of striated planes and their

associated slicken sides were measured. Analysis of the brittle micro-faults using a computer-aided method resulted in the definition of the tectonic paleostress tensors responsible for their formation. A first brittle compression characterized by a maximum compressive stress σ_1 predominantly trending N 15^o E was mainly identified along the NE-SW striking major fractures. This particular brittle tectonic event is believed to be related to the sinistral Cretaceous reactivation of Pan Africa NE-SW transcurrent faults. In general, all the estimated stress tensors close to strike-slip tensor are characterized by a significant deflection of the direction of the maximum compressive stress σ_1 ranging N 180^o E to N 60^o E. By comparing these data with micro-tectonic and mathematical models on strike-slip faults is particularly demonstrated. A second N 15^o E compressive brittle event is also observed.

Ajakaiye *et al*. (1991) interpreted the aeromagnetic survey of substantial part of Nigeria carried out by the Geological Survey of Nigeria between 1974 and 1980. The results of their analysis reveals magnetic lineation and regions of distinct magnetic interpretations character and field level which are interpreted as expressions of tectonic features related to igneous intrusives of various ages. Classical analytical techniques were adopted for upward and downward continuation, frequency domain filtering of the data, and for the interpretation of surface and subsurface structures in the area.

Likkasson *et al*. (2005) interpreted the 24 aeromagnetic maps covering the middle Benue Basin. He subjected the data from the middle Basin to map and profile analysis using analytic signal, matched filtering and forward/inverse modeling as processing tools to the aeromagnetic total-field intensity anomaly of the Middle Benue Trough. Magnetic depth to geology contrast or faults for the sedimentary cover gives a maximum of 3.30 km from the ground level. The spectral matching

yielded three dipole equivalent source layers at 0.89, 4.33 and 18.22 km depth. Depth of 4.33 km corresponds to maximum thickness of sediment, while that of 0.89 km may be attributable to effects of survey terrain clearance and other shallow plate sources. He attributed the magnetic layer of 18.22 km to correspond to the base of the curve depth in the area. Results obtained from selected values of susceptibility from the sediments, metamorphic and granite basement and basic intrusions give sedimentary thickness along the three profiles across the area up to 4.5 km with more filting depth on the River Benue zone.

All the studies described above are limited in coverage and depth with respect to the various methods used. They however, indicate the need for a detailed study of the Borno basin so as to ascertain its structure, tectonic evolution and origin.

CHAPTER THREE

3.0 MATERIALS AND METHODS

During this research work, different software in accordance with the task at hand were used for data capturing, image processing to enhance image, delineate features gridding and mapping programs to grid and map aeromagnetic data. Word processing, spread sheet and database software were also used. Examples of software and hardware used are:

i. Eight (8) aeromagnetic maps number's 22, 23, 24, 43, 44, 45, 65 and 66 covering parts of the study area.
ii. One personal computer and laptop with good speed and large memory.
iii. Different printers (White and Coloured), plotters and scanner.
iv. Surfer package version 8.0

v. Oasis Montaj software.

vi. Transparent papers and stationeries.

3.1 Data Collection

Aeromagnetic survey of a substantial part of Nigeria was carried out by the geological survey of Nigeria between 1974 and 1980. The magnetic information consists of profiles or flight lines plotted on continuous strip chart or tape records. To achieve this, the Nigeria landmass was divided into blocks. The magnetic data were collected at a nominal flight altitude of 152.4 m along N-S flight lines spaced approximately 2 km apart. The aeromagnetic survey measured only the total field, F. The data were later published in the form of $^1/_2{}^o$ by $^1/_2{}^o$ aeromagnetic maps on a scale of 1: 100 000. The magnetic values were plotted at 10nT (gamma) interval. Eight (8) aeromagnetic maps with maps numbers 22, 23, 24, 43, 44, 45, 65 and 66 were used for the study area. Each map was digitized on a 1.5 x 1.5 km^2 grid system.

3.2 Digitization and Collation of Data

The data used for this research were collected from the aeromagnetic maps covering the parts of Borno basin. This is because the original data on tapes could not be obtained. Two methods can be used for map digitization (Udensi, 2001). These are:

i. Digitization along flight lines

ii. Digitization on grid layout

The later was applied because:

i. The study area is occupied by dense magnetic contours.

ii. The computer packages which was used for data analysis requires that the data be supplied on an even grid system.

The contour lines of the said maps were dense thereby reducing errors of human judgement associated with visual interpolation method.

Each map was digitized on a 1.5 x 1.5 km^2 grid system. This spacing imposes a Nyquist frequency of $^1/_3$ km^{-1}. Thus the narrowest magnetic feature that can be defined by the digitized data has a width of 3 km. Previous study with crustal magnetic anomalies (Udensi, 2001) shows that this spacing is more than suitable for the portrayal of and interpretation of magnetic anomalies arising from regional crustal structure, which are much wider than 6 km and therefore

lie below the frequency range for which computational errors arising from aliasing do not occur.

After digitizing each aeromagnetic map, the data were collected and recorded in 19 by 19 coding sheets. Each sheet contains a record of the boundary longitudes and latitudes, the maps number and name of the town over flown.

The values obtained were then re-contoured and the resulting map was compared with the original map. This helped the researcher to correct whatever error that has been introduced during digitization.

3.3 The Production of Dataset (Super Data)

The next stage of the study was to produce a unified aeromagnetic map of the study area. This is the map that would be the subject of analysis and interpretation.

Figure 3.1 is the method of eliminating edge effect in super map. The first step in the production of the unified aeromagnetic map (super map) of the parts of Borno Basin is the production of a combined magnetic dataset for the area.

The first problem to overcome is that of boundary (edge) effect, which must be overcome before the super data is produced.

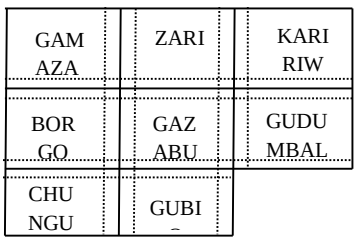

Figure 3.1: Method of Eliminating Edge Effect in Super Map.

Each small map, which is represented by the map number, contains 19 by 19 digitized magnetic values. At the boundary of two maps for example, maps 22 and 23 the field values in the last column of map (22) has the same coordinates (latitude and longitude) as the field values in the first column of map (23). Also at the boundary between map (22) and (43) (for example), the field value at the last row of map (22) has the same coordinates as the field values in the first row of map (43). To have a data set therefore, all the magnetic values with same coordinates must be added and averaged so that there would be rows and columns of magnetic points with the same coordinates.

There are two ways through which this task could be achieved. A computer program can be designed to achieve the aim where one is dealing with large numbers of maps say from ten upwards. But when dealing with maps below ten, then manual manipulation is adequate though care has to be taken not to run into unnecessary errors, which could be fatal in its implications.

For this work, manual coupling was adopted and it was very adequate, it will be observed that the values that are to be merged are almost equal which an indication of good digitization is.

As earlier explained, when the last column and the first column of the adjoining map is average, the new data value generated is recorded in place of the initial data value, the same process is

repeated for the rows between two maps. A total number of 3 025 data values were obtained as the super data covering the entire study area.

3.4 Production of the Composite Aeromagnetic Map of the Study Area

The dataset (super data) obtained in the last section (3.4) cannot yet be contoured because the coordinates (latitude and longitude) of each of the data points are yet to be supplied. To obtain this, simple computer program in Basic language was used in reading the data points row by row and calculating their latitude and longitude-using base values already supplied. The output obtained is in the form of column of X, Y, Z, where X, Y and Z represent longitude, latitude and magnetic value of the given data point respectively. The dataset that is obtain from the computer program is tagged “Tona.Dat” to identify it different from the previous super data.

The “Tona.Dat” obtained, which is in a three dimensional coordinate form X, Y, Z is the form the data must be so as to be acceptable to a contouring package SURFER. SURFER is a menu driven interactive computer program which places each magnetic data accordingly and thereafter produces a contour map, which is the unified Aeromagnetic Map.

Figure 3.2 is the Total Magnetic Intensity Map of parts of Borno Basin, which was later produced at a lower gridding and contoured at 20 nT intervals. This was done so that the contour lines would be shown clearly. The contour values shown in Figure 3.2 ranges from 7 740 nT to 7 800 nT after the base value of 25 000 nT has been removed from all data points. Figure 3.2 is the map that would be used for analysis and interpretation. Figure 3.3 is the Total Magnetic Intensity map of parts of Borno basin generated in Oasis Montaj software.

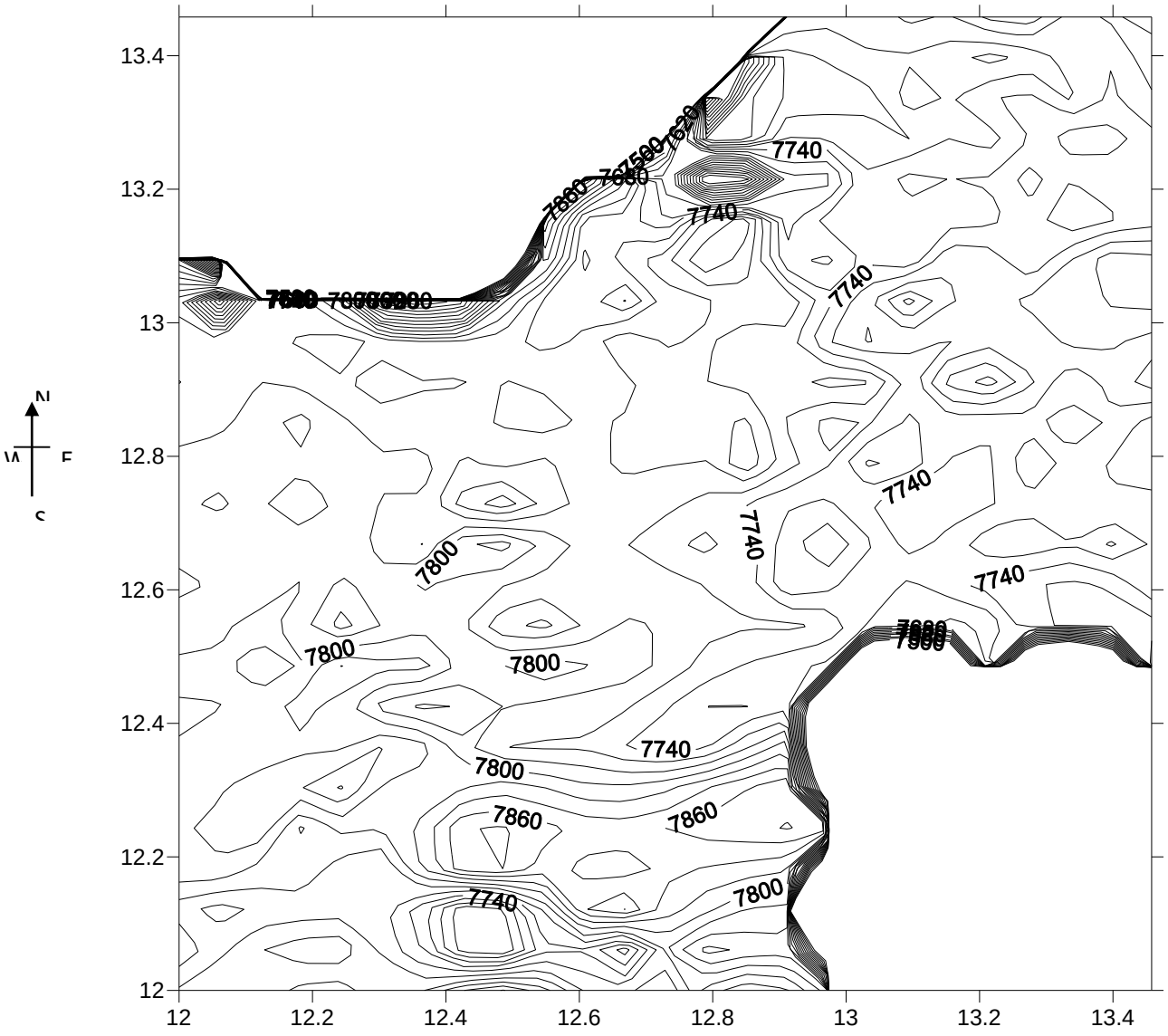

Figure 3.2: Total Magnetic Intensity Map of Parts of Borno Basin Using Surfer package version 8.0

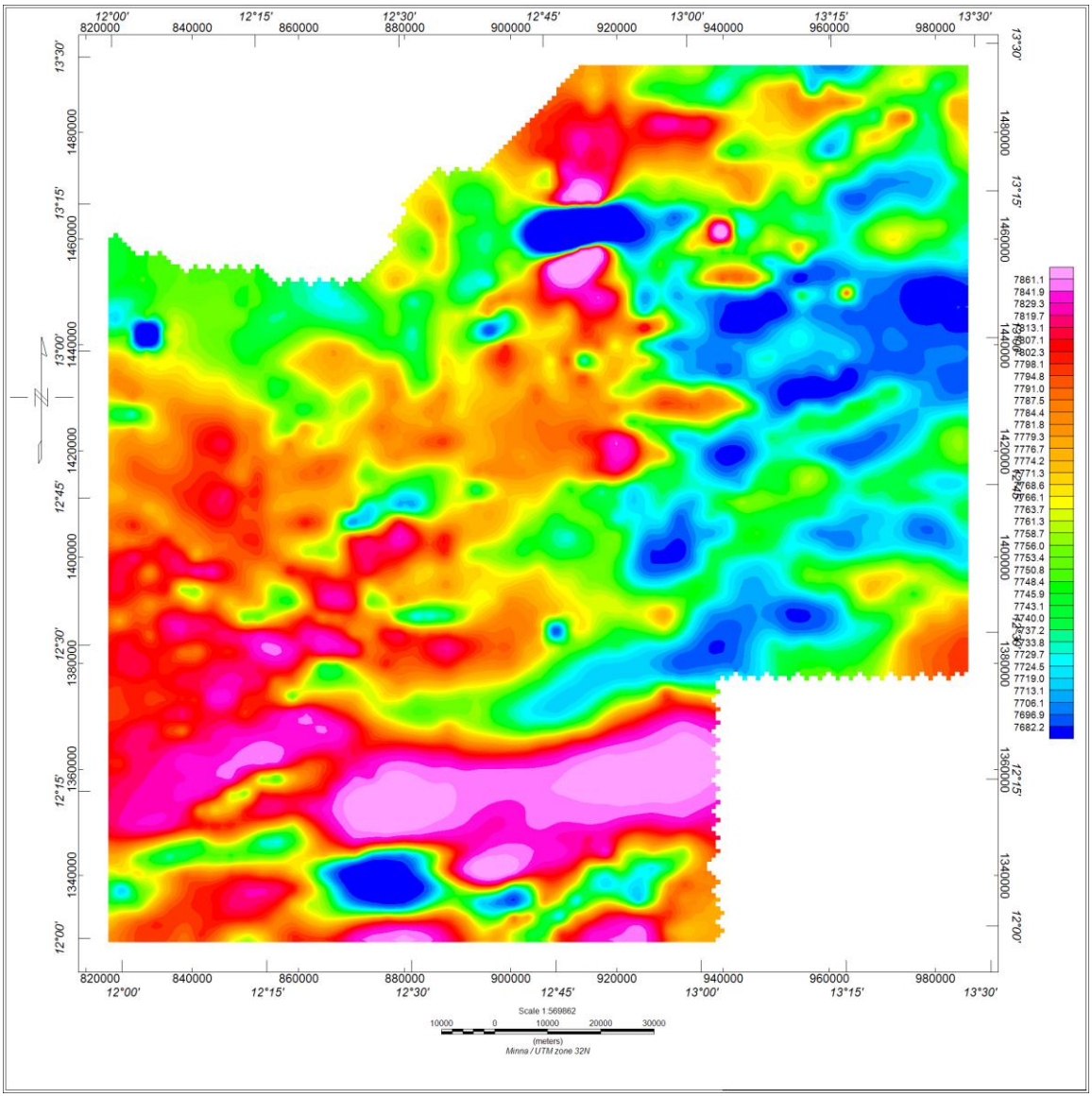

Figure 3.3: Total Magnetic Intensity Map of Parts of Borno Basin generated in Oasis Montaj software

For potential field data to be interpreted, the residual anomalies must be separated from the regional (background) field. The polynomial fitting method is about the most flexible and most applied of the analytical method for determining regional magnetic field (Skeels, 1967; Johnson, 1969 and Dobrin, 1976). In this method, the matching of regional by a polynomial surface of low order exposed the residual features as a random error. The treatment is based on statistical theory. The observed data were used to compute, usually by least squares, the mathematically describable surface giving the closest fit to the magnetic field that can be obtained within a specified degree of detail. It was assumed reasonably that the regional field is a first degree polynomial surface. All the regional fields were therefore calculated as two dimensional (2-D) first degree polynomial surfaces. A computer program was used to derive the residual magnetic values by subtracting values of the regional fields from the total magnetic values at the grid cross point. The resultant map is shown in Figure 3.4. The regional map trends NW-SE. The regional trend is attributed to effects, of deeper heterogeneity of the earth crust. The trend agrees completely with the deductions of Ajakaiye *et al*. (1981) who identified a system of NW-SE trending narrow magnetic lineaments along which are concentrated the Alkaline Ring complexes and suggested that the lineament represented pre-existing zones of weakness in the pan African crust. Ananaba *et al*. (1987) also identified predominant tectonic trends in the NW-SE and N-S directions over the present study area in particular and other parts of the Northern Nigeria in general.

A computer program (SPT) was used to derive the residual magnetic values by subtracting values of the regional field from the total magnetic value at the grid cross points.

Figure 3.5 shows that the magnetic residual values range from -60.00 to 60.00. Negative residual dominates the study area because the area is close to the magnetic equator.

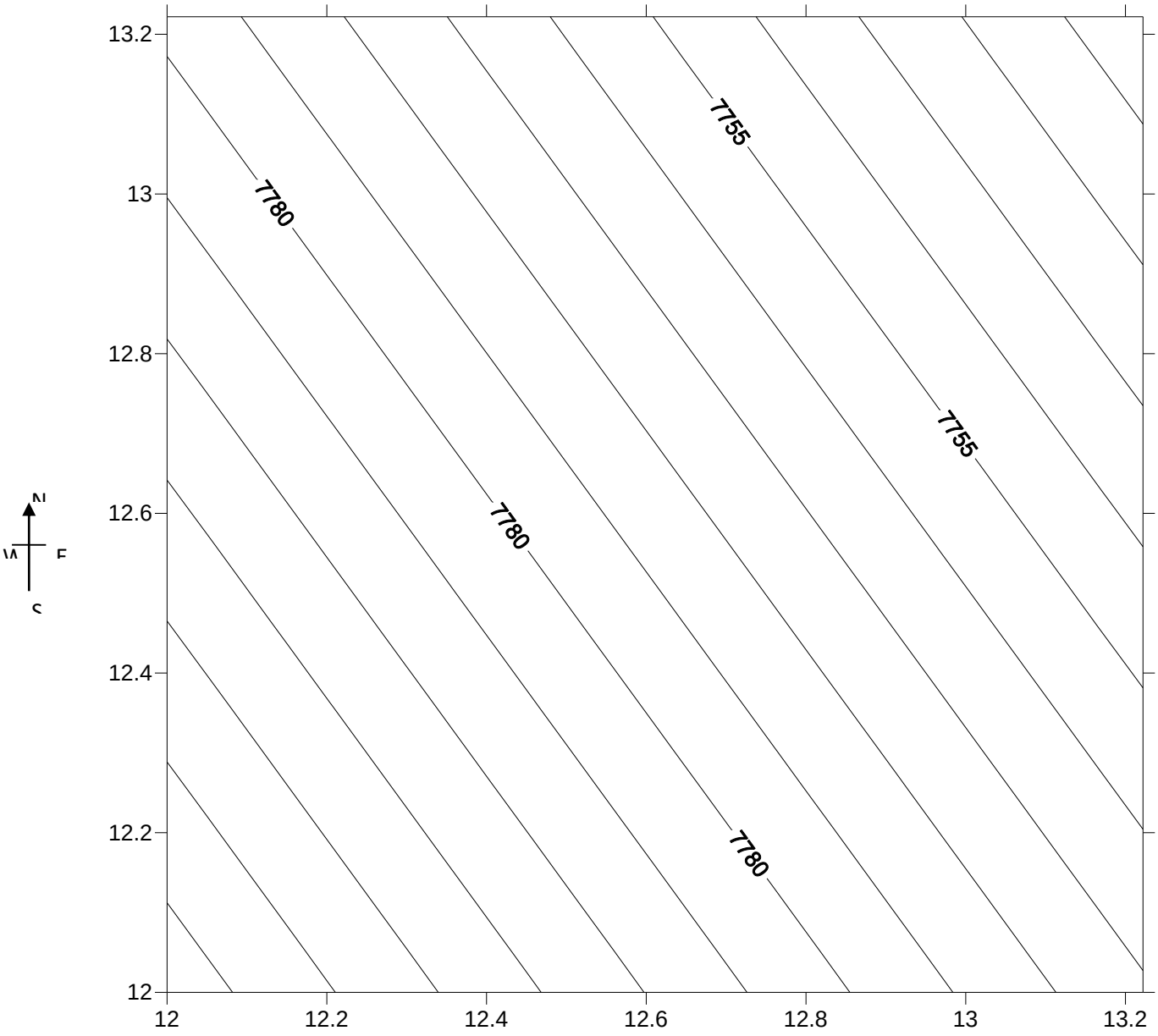

Figure 3.4: Regional Map of Parts of Borno Basin Showing the NW-SE Trend, Vertical and Horizontal Axis in Degrees.

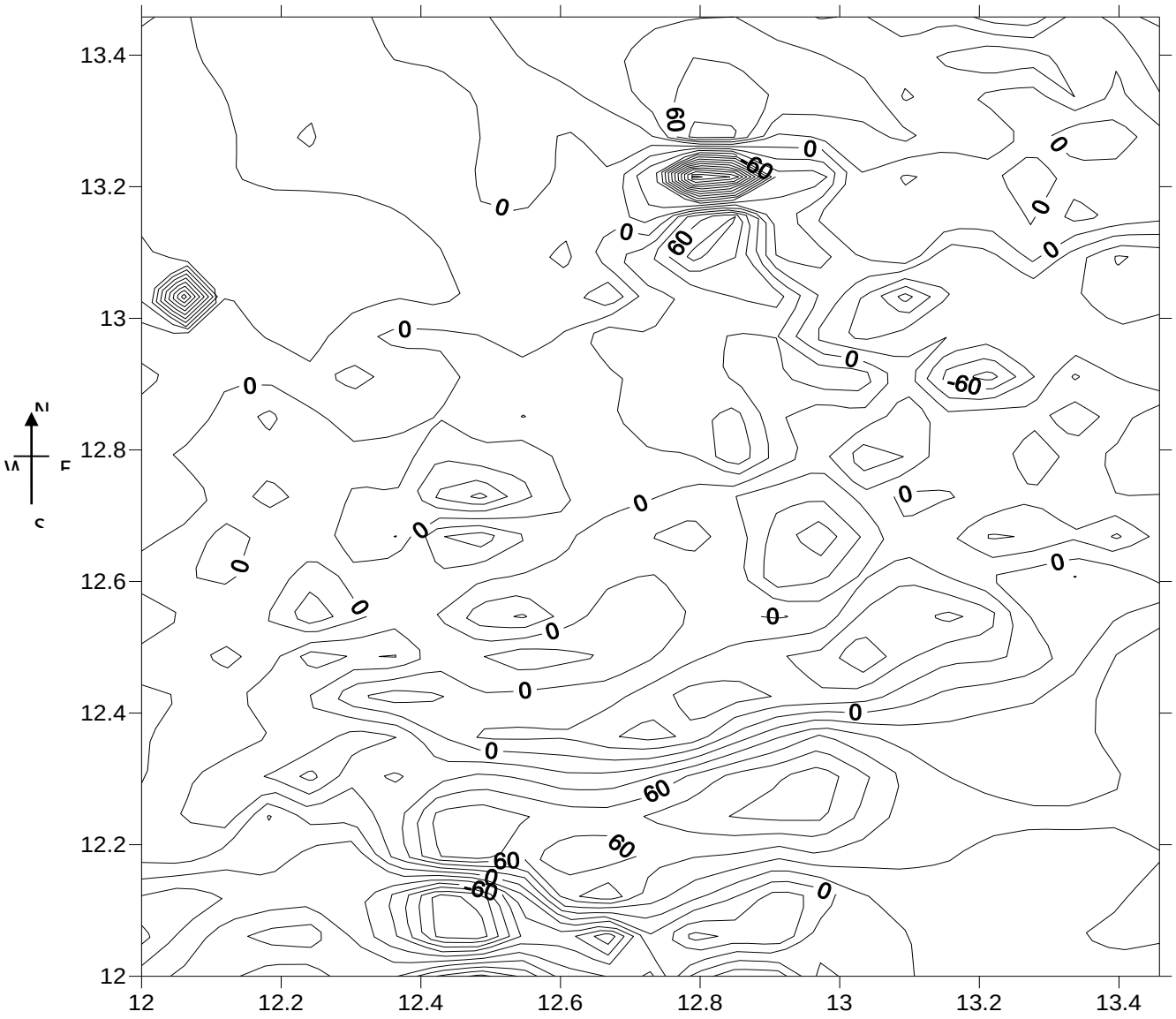

Figure 3.5: Residual Magnetic Map of Parts of Borno Basin Contoured at Intervals of 10 nT, Vertical and Horizontal Axis in Degrees.

3.5 Spectral Analysis of the Residual Field

The word 'spectrum' (the plural of which is 'spectra') is used today to mean 'a display of electromagnetic radiation as a function of wavelength.' Spectrum used to mean 'phantom' or 'apparition', but Isaac Newton introduced a new meaning in 1671, when he reported his experiment of decomposing the white sunlight into colors using a prism (Lochner *et al*., 2010).

One of the principal applications of aeromagnetic data is in the determination of depth to buried magnetic rocks. These depths are commonly computed from measurements made on the widths and slopes of individual anomalies of the aeromagnetic profiles. If adequate grid control is available, the use catalogues of three-dimensional prismatic models can also establish depths (Lochner *et al*., 2010).A frequent shortcoming of these techniques is the fact that the calculations are performed on isolated anomalies, which are distorted by noise and recognized recently that a statistical approach may sometimes be preferable because more than one anomaly can then be used to determine depths to magnetic structures (Lochner *et al*., 2010). While this approach cannot be expected to have the resolution theoretically achievable by analysis carried out on individual anomalies, it can lead to the determination of mean depth values to major units of buried magnetic rocks (Lochner *et al*., 2010).

The evolution of spectral analysis has same important precursor, by which one tried to present data only in a simple time-domain style. The most important of these precursors is the harmonics analysis of Fourier series expansion of a given time series of data.

According to Fourier's theory, any function f (*t*) satisfying certain restrictions, can be expressed as a sum of an infinite number of sinusoidal terms (Lochner *et al*., 2010).

In the general case f (*t*) can stand for any time function, such as displacement particle velocity, acceleration, temperature, rainfall, wind velocity, geomagnetic field intensity. The geomagnetic

field can also be a space function f (x). In this study, the characteristics of the residual magnetic field is studied using statistical spectral method. This is done by first transforming the data from space to the frequency domain and then analyzing their frequency characteristics.

3.6 Fundamentals of Spectral Analysis

3.6.1 Waveforms

The waveform of a sound is a graph of the way the pressure changes between the wavefronts. This is usually a very convoluted pattern and the actual sound of the wave is not apparent when looking at the waveform. As a matter of fact, the waveform does not usually repeat exactly from one cycle to another.

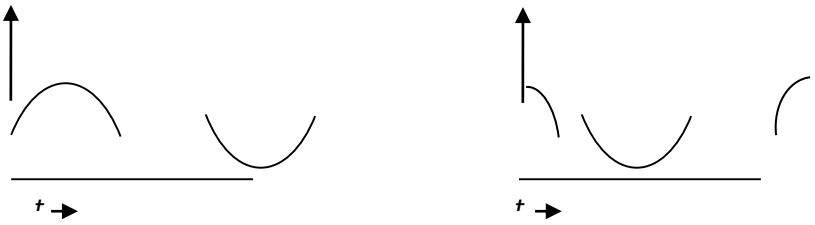

sine function cosine function

Figure 3.6: Sine and cosine functions

The waveform produced by simple harmonic motion is the SINE WAVE. We graph a sine wave by plotting the function:

$$f(t) = A\sin 2\pi ft \tag{3.1}$$

To do this we divide up our graph paper horizontally into equal chunks to represent a time scale, and for each time, t we want to plot, we multiply t by $2\pi f$ (f is frequency) and look up the sine of the result. That sine value is what gets used for the vertical part of the graph. There is also a function called a cosine wave. The expression is

$$f(t) = A\cos 2\pi ft \tag{3.2}$$

and it looks just like the sine wave. The difference is that the cosine of an angle is equal to the sine of an angle 90 degrees bigger. When we have two waveforms which have the same shape and frequency but are offset in time, we say they are out of phase by the amount of angle you have to add to the $2\pi ft$ term of the first to move them together. In other words, the wave defined by $\sin 2\pi ft$ is out of phase with the wave defined as $\sin 2\pi ft$ by the angle p.

The second simplest waveform is probably the combination of two sine waves. Any combination of waves is interpreted by the ear as a single waveform, and that waveform is merely the sum of all of the waves passing that spot. Here are a few rules about the addition of two sine waves:

i. If both have the same frequency and phase, the result is a sine wave of amplitude equal to the sum of the two amplitudes.

ii. If both have the same frequency and amplitude but are 180 degrees out of phase, the result is zero. Any other combinations of amplitude produce a result of amplitude equal to the difference in the two original amplitudes.

iii. If both are the same frequency and amplitude but are out of phase a value other 180 degrees, you get a sine wave of amplitude less than the sum of the two and of intermediate phase.

iv. If the two sine waves are not the same frequency, the result is complex. In fact, the waveform will not be the same for each cycle unless the frequency of one sine wave is an exact multiple of the frequency of the other.

If the combinations of more than two sine waves were employed, it will be discover that the waveforms become very complex indeed, and depend on the amplitude, frequency and phase of each component. Every stable waveform you discover will be made up of sine waves with frequencies that are whole number multiple of the frequency of the composite wave.

3.6.2 Fourier Analysis

The reverse process has been shown mathematically to be true. Any waveform can be analyzed as a combination of sine waves of various amplitude, frequency and phase (artisites.ucsc.edu/ems/music/tech_background/TE-04/teces_04.html). The method of analysis was developed by Fourier in 1807 and is called Fourier Analysis.

The actual procedure for Fourier analysis is too complex to get into here, but the result (with stable waveforms) is an expression of the form:

$$A\sin\varpi t + B\cos\varpi t + C\sin 2\varpi t + D\cos 2\varpi t + E\sin 3\varpi t \qquad (3.3)$$

and so forth. The omega (looks like a w) represents the frequency in radians per second, also known as angular frequency. The inclusion of cosine waves as well as sine waves takes care of phase, and the letters represent the amplitude of each component. This result is easily translated into a bar graph with one bar per component. Since the ear is apparently not sensitive to phase, we often simplify the graph into a sine waves only form.

The lowest component of the waveform is known as the FUNDAMENTAL, and the others are HARMONICS, with a number corresponding to the multiple of the fundamental frequency. The second harmonic is twice the fundamental frequency, the third harmonic is three times the fundamental frequency, and so forth. It is important to recognize that the harmonic number is not the same as the equivalent musical interval name, although the early harmonics do approximate some of the intervals. The most important relationship is that the harmonics numbered by powers of two are various octaves.

Non-repeating waveforms may be disassembled by Fourier means also, but the result is a complex integral that is not useful as a visual aid. However, if we disregard phase, these waveforms may also be represented on a spectral plot as long as we remember that the components are not

necessarily whole number multiples of the fundamental frequency and therefore do not qualify as harmonics.

We should not say that a non-harmonic waveform is not pitched, but it is true that the worse the spectral plot fits the harmonic model the more difficult it is to perceive pitch in a sound. There are sounds whose waveforms are so complex that the Fourier process gives a statistical answer, (these waveforms are the sounds commonly called noise). The likelihood of finding a particular frequency can be expressed as a component over a large enough time, but any component cannot be assign constant amplitude. To describe such sounds on a spectral plot, we plot the probability curve. A very narrow band of noise will sound like a pitched tone, but as the curve widens, we lose the impression of pitch, aware only of a vague highness or lowness of the sound. Noise that spreads across the entire range of hearing is called WHITE NOISE if it has equal probability of all frequencies being represented (artisites.ucsc.edu/ems/music/tech_background/TE-04/teces_04.html). Such noise sounds high pitched because of the logarithmic response of the ear to frequency. (Our ears consider the octave 100 Hz to 200 Hz to be equal to the octave 1 000 Hz to 2 000 Hz, even though the higher one has a much wider frequency spread, and therefore more power). Noise with emphasis added to the low end to compensate for this is called PINK NOISE (artisites.ucsc.edu/ems/music/tech_background/TE-04/teces_04.html).

3.7 Energy Spectrum and Depth of Magnetic Source

Consider the energy spectrum of the total magnetic field intensity anomaly over a single rectangular block. The expression for the energy spectrum transcribed in polar coordinates is given as follows. (Spector and Grant, 1970)

$$\text{If } r = (u^2 + v^2) \text{ and } \theta = \arctan\left(\frac{u}{v}\right) \tag{3.4}$$

Then the energy spectrum E (r, θ) is given by

$$E(r,\theta) = 4\pi^2 k^2 e^{-2hr}\left(1 - e^{-tr}\right)S^2(r,\theta)R^2T(\theta)R^2k(\theta) \tag{3.5}$$

Where $^{K}/_{4ab}$ is the magnetic moment per unit volume of the rectangular block, a and b are the width and length, K is the magnetic moment per unit depth.

$$S(r,\theta) = \frac{\sin(ar\cos(\theta))}{ar\cos\theta}\frac{\sin(br\cos(\theta))}{br\cos(\theta)} \tag{3.6}$$

$$R_{T^2}(\theta) = \left[n^2 + (1\cos(\theta) + M\sin(\theta)\right]^2 \tag{3.7}$$

L, m, n are direction cosines of the magnetic moment vector.

For the purpose of analyzing aeromagnetic maps, the ground is assumed to consist of a number of independent ensembles of rectangular, vertical sided parallel piped, and each ensemble is characterized by a joint frequency distribution for the depth, h, width, a, and length, b and depth - extent, t.

According to this hypothesis, the map of the magnetic field intensity over an area, after the removal of the main geomagnetic component, is assumed to consist of the superposition of a large number of individual anomalies most of them over lapping, which are caused by several ensembles of blocks having various dimensions and magnetizations.

Making further assumption that for a moderately large number of bodies, the average values of inclination and declination of the magnetic vector will not differ appreciably from the inclination and declination of the geomagnetic field, Spector and Grant (1970) obtained the expression for the ensemble average of the radial spectrum as

$$< ECr> = 4K\pi^2K^2>\lambda^{-2hr}>< (1 - \lambda^{-tr})^2>< S^2(r)> \tag{3.8}$$

$$< S^2(r) >= \frac{1}{\pi}\int_0^n < S(r,\theta) > d\theta \tag{3.9}$$

The ensembles average depth, h enters only into the factor.

$$<\lambda^{-2hr}> = \frac{\lambda^{-2hr} \sin h(2r\Delta h)}{4r\,\Delta h} \qquad (3.10)$$

For depth estimates for magnetic field data, this can be approximated to exponential (-2hr) (Spector and Grant, 1970). The exponential (-2hr) term is the dominant factor in the power spectrum. Map spectral are usually declining functions of r whose rate decay is largely dominated by the mean depth of bodies. If these are two set of sources, then they can be recognized by marked change in the spectral decay rate. The energy spectrum of the double ensemble will then consist of two parts. The first, which relates to the deeper sources, is relatively strong and at low frequencies and decays away rapidly. The second, which arises from the shallower ensemble of sources, dominates the high frequency end of the spectrum. In the general case, the radial spectrum may be conveniently approximated by straight line segments, the slopes of which relate to depths of the possible layers (Hahn *et al*., 1976, Spector and Grant, 1970).

The residual total magnetic field intensity values are used to obtain the two dimensional Fourier Transform from which the spectrum is to be extracted from the residual values T (x, y) consisting of M rows and N Columns in the X – Y plane, the two dimensional Fourier Transform is obtained. The evaluation is done using an algorithm that is a two dimensional extension of the fast Fourier Transform. Next, the frequency intervals are subdivided into sub-intervals, which lie within one unit of frequency range. The average spectrum of the partial waves falling within this frequency range is calculated and the resulting values together constitute the redial spectrum of the anomalous field (Hahn *et al*., 1976, Udensi, 2001).

Finally we plot the logarithm of the energy values versus frequency on a linear scale and locate the linear segments.

Each linear segment groups points due to anomalies caused by bodies occurring within a particular depth. If Z is the mean depth of a layer, the depth factor for this ensemble of anomalies is exponential (-2ZK). Thus the logarithmic plot of the radial spectrum would give a straight line whose slope is -2Z. The mean depth of the buried ensemble is thus given as

$$Z = -m/2 \tag{3.11}$$

Where m is the slope of the fitting straight line. Equation (3.11) can be applied directly if the frequency unit is in radians per kilometer. If, however, the frequency unit is in cycles per kilometre the corresponding relation can be expressed as

$$Z = -m/4 \tag{3.12}$$

The use of Discrete Fourier Transform introduced the problem of aliasing and the truncation effect (or Gibbs phenomenon). Aliasing was reduced by the digitizing interval used in the study. The truncation effect arises in that when a limited portion of an aeromagnetic anomaly map is subjected to Fourier synthesis, it difficult to reconstruct the sharp edges of the anomaly with a limited number of frequencies. This truncation leads to the introduction of spurious oscillations around the region of discontinuity. This means that false frequencies will be introduced into the spectrum. Applying a cosine-taper to the observed data before Fourier transformation will reduced the truncating effect. Finally, it has been found (Pal *et al*., 1978) that in the use of the approach to magnetic source depth determinations, the error in the depth prediction increases with the depth of source and is also related to the map size. The map size required for adequate results should be much larger (about 10 time) than the target depth. The low frequency components in the energy spectrum are generated from the deepest layers whose locations are most likely in error. Thus it is advisable in the general

method here to ignore the first few points in the energy spectrum. The Spector and Grant (1970) method described above, as noted earlier assumes a uniform distribution of parameters for an ensemble of magnetized blocks to a depth – dependent. This led to exponential rate of decay shown in equation (3.8).

3.8 Upward Continuation

This is a tool employed in gravity interpretation to determine the form of regional gravity variation over a survey area, since the region field is assumed to originate from relatively deep seated structures. Upward continuation attenuates the high–wavenumber anomalies of the deeper-seated sources (Kearey *et al*., 2001).

Downward continuation of potential fields is of more restricted application. It is used in the resolution of the separate anomalies caused by adjacent structures whose effects overlap at the level of observation (Kearey *et al*., 2001).

A potential field measured on a given observation plane at a constant height can be calculated as though the observations were made on a different plane, either higher (upward continuation) or lower (downward continuation). The equation of the wavenumber domain filter to produce upward continuation is simply:

$$F = e^{-hw} \tag{3.13}$$

Where h is the continuation height. This function decays steadily with increasing wavenumber, attenuating the higher wavenumbers more severely, thus producing a map in which more regional features predominate. Some careful experimentation is usually necessary to obtain acceptable results (Reeves, 2005).

CHAPTER FOUR

4.0 RESULTS AND DISCUSSIONS

4.1 Structural Trends

The contour map Figure 4.1, shows the northern part with a predominantly NW-SE trending. This trend is observed down to latitude 12.1^{o}. At mid portion of the map between latitude 12.7^{o} down to 12.4^{o}, the trend changes to E-W. From latitude 12.1^{o} downwards, the trend changes to NE-SW which continues to the end of the map.

Thus, the NW-SE trend at the top part of the map and NE-SW trend at bottom part, can be related to what Wright (1968) and Ball (1980) have also identified as a system of NE-SW and NW-SE conjugate pair of fractures which exist everywhere within the Pan Africa Mobile Belt. These have been attributed to brittle the deformation during the later part of Pan Africa Orogeny.

4.2 Magnetic Closures

Several magnetic closures both lows or highs dot the study area as shown in Figure 4.1. The closure of magnetic lows are marked (L), while the closure of magnetic highs are marked (H). Most of these closures are prominent both at the edges and middle of the map Figure 4.1. Towards the southern part of the map between latitudes 12^{o} to 12.7^{o} and longitudes 12^{o} to 12.9^{o} are sets of magnetic highs which are elliptical in shape. Also, at the top and at the eastern portion of the map, several magnetic lows are observed between latitude 12.6^{o} to 13.4^{o} and longitude 12.9^{o} to 13.5^{o}.

4.3 Magnetic Discontinuities

There are no major discontinuities observed on the map except two short such discontinuities which close observation reveals one of such is latitude 12.3^{o} which runs SW-SW trending. Another one runs S-W bottom of the map on latitude 12.1^{o}. These discontinuities are indicated as X-X' and Y-Y' in Figure 4.1.

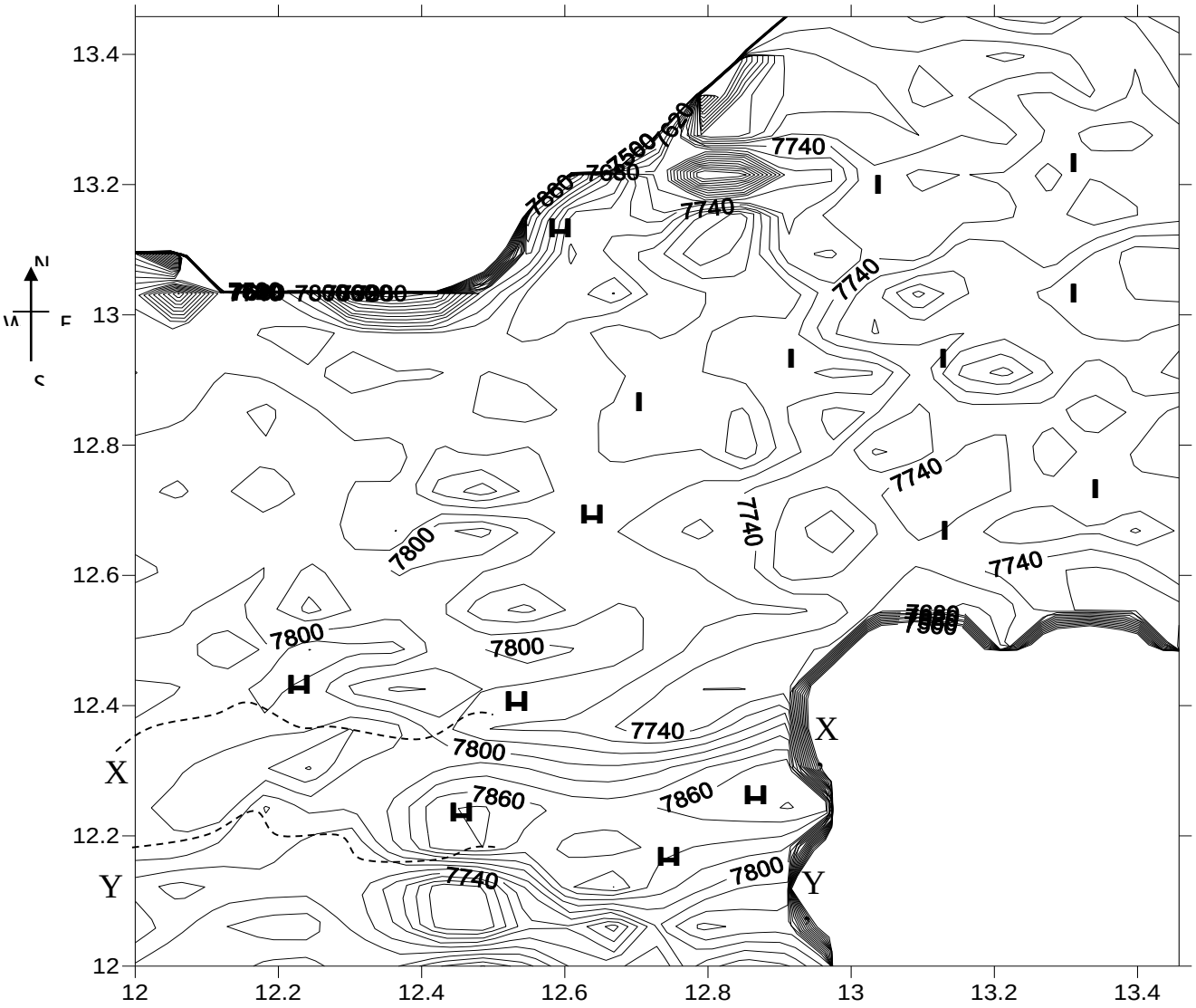

Figure 4.1: Composite Aeromagnetic Map of Parts of Bornu Basin Showing Magnetic Lows (L) and Highs (H), Discontinuities (XX' and YY') Contour interval is 20 nT, vertical and horizontal axis in degrees.

4.4 Spectral Depths

The research area covering between latitude12^{o} N to 13^{o}5' N and longitude 12^{o} E to 13^{o}5' E subdivided into sixteen (16) sections for the purpose of spectral depth determination.

Graphs of the logarithm of the spectral energies against frequencies obtained for the various sections are shown in appendix B. The gradient of each of the line segments were evaluated. Depth to basement are then evaluated using $Z = -m/2$ equation (3.11), where m represents the gradient and Z gives the mean depth of buried assemblage.

For this analysis, the study area is divided into sixteen (16) sections allowing spectral depth determination at every 15 km by 15 km interval of the field. These depths were shown as h_1 and h_2 on Table (4.1), from the table, the first layer depth varies in thickness from 0.18 km minimum to 0.37 km maximum, and has an average thickness of 0.28 km. The second layer (h_2) depth varies from a thickness of 1.79 km minimum to 5.34 km maximum and has an average depth of 2.99 km.

Figure 4.2 depict first layer h_1 depth contoured at an interval of 20 metres vertical and horizontal axes in degrees. The high depth is at the central region which is, area on the map with light pink colour, while the low depths with deep pink colour are at the surrounding edges of North, South and Eastern part of the map. Figure 4.3 depict the Surface plots of first magnetic layer.

Figure 4.4 depict second layer h_2 depth contoured at an interval of 50 metres vertical and horizontal axes in degrees. The high depths in light blue colour are seen in the North and Southern region, while the low depths with deep blue colour are found at the Eastern and central part of the map. Figure 4.5 depict the Surface plots of second magnetic layer.

Table 4.1: Depth Estimate, Location for the first and Second Layers

SECTION	LONGITUDE (^{o})	LATITUDE (^{o})	h_1 (km)	h_2 (km)

1	12.50	12.50	0.29	2.50
2	12.50	13.00	0.33	1.79
3	13.00	12.50	0.34	3.75
4	13.00	13.00	0.26	5.34
5	12.75	12.25	0.28	2.82
6	12.75	12.75	0.18	2.43
7	12.75	12.25	0.22	3.75
8	12.25	12.75	0.37	2.50
9	12.75	12.75	0.25	5.00
10	13.25	12.75	0.31	1.82
11	12.50	12.25	0.29	3.09
12	12.50	12.75	0.24	3.50
13	12.50	13.25	0.29	2.11
14	13.00	12.25	0.31	2.73
15	13.00	12.75	0.27	2.50
16	13.00	13.25	0.29	2.13

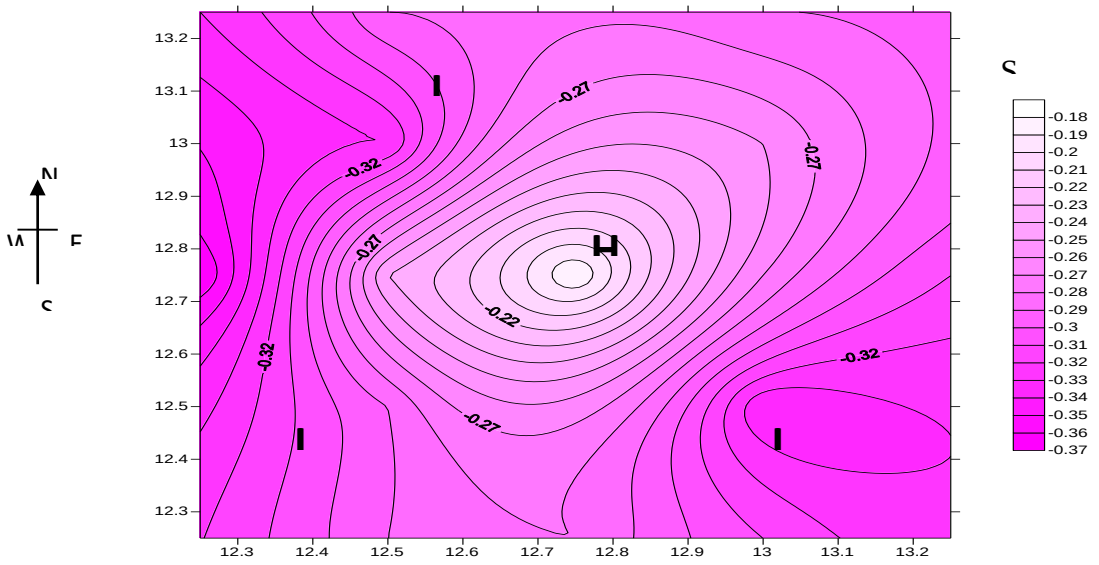

Figure 4.2: First Layer h_1 Depth contoured at an interval of 20 metres vertical and horizontal axes in degrees.

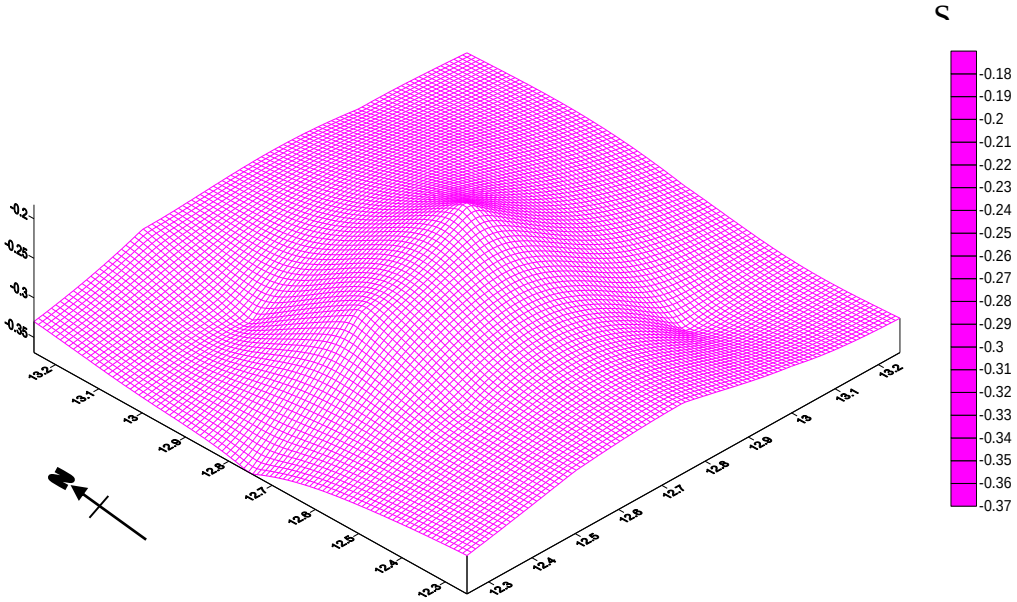

Figure 4.3: Surface Plots of First Magnetic Layer

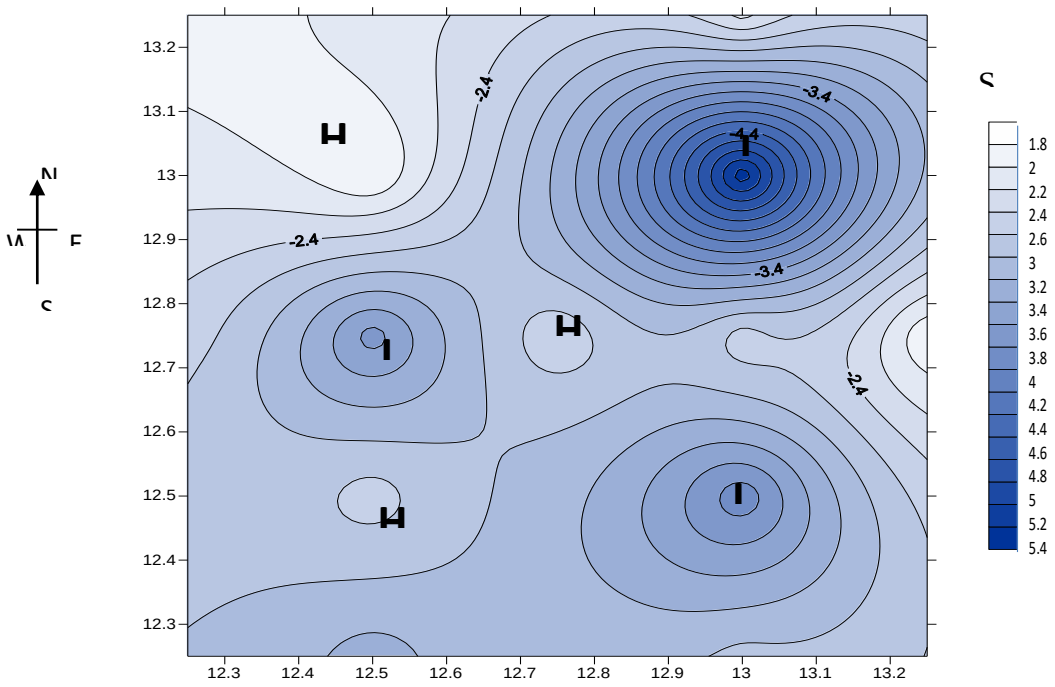

Figure 4.4: Second Layer h_2 Depth contoured at an interval of 50 metres vertical and horizontal axes in degrees.

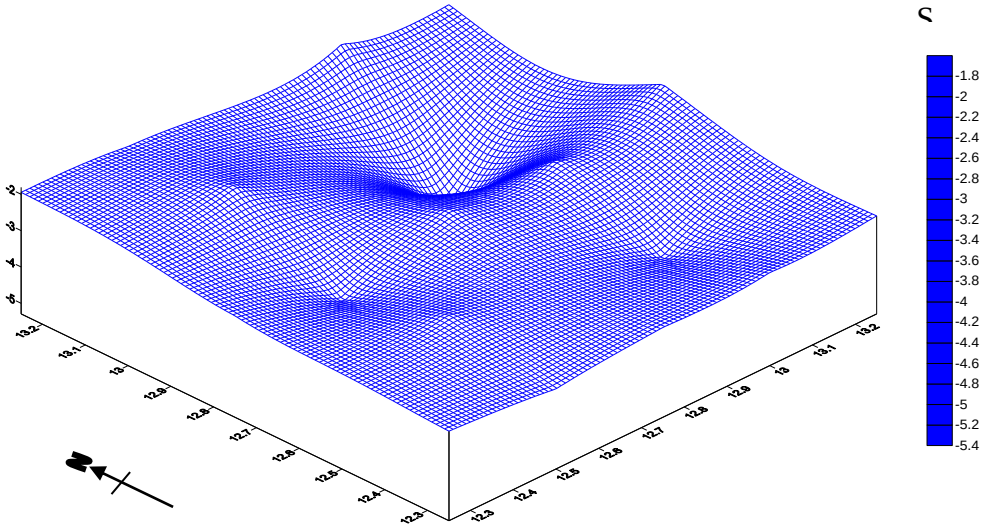

Figure 4.5: Surface Plots of Second Magnetic Layer

Upward continuation is considered a clean filter because it produces almost no side effects that may require the application of other filters or processes to correct. Because of this, it is often used to remove or minimize the effects of shallow sources and noise in grids.

Upward continuation was used for the purpose of this research work. Figures 4.6, 4.7, 4.8, 4.9, 4.10 and 4.11 depict the upward continuation filtering method of the total magnetic intensity map of parts of Borno basin used for separating causative sources from various depths ranging from 1 km, 2 km, 3 km, 5 km, 7.5 km and 10 km respectively.

Close observation at Figure 3.3 the total magnetic intensity map of parts of Borno basin generated in Oasis Montaj software and Figures 4.6, 4.7, 4.8, 4.9, 4.10 and 4.11 upward continuations of the total magnetic intensity map of parts of Borno basin 1 km, 2 km, 3 km, 5 km, 7.5 km and 10 km respectively, reveals that the local disturbances are completely filtered.

Figure 4.11 being the most refine map of upward continuation of the total magnetic intensity map of parts of Borno basin reveals that the thickness of sediment basin is at northeastern part of the map between latitude12^{o}45’ to 13^{o}15’ North and longitude 13^{o}00’ to 13^{o}30’ East (Raeburn and Jones (1934), Matheis (1976), Avbovbo *et al.* (1986), Bellion, 1989).

The pink colour has the lowest magnetic intensities (7 808.9 nT) showing that the sedimentary cover is tin while the deep blue colour is the regional feature being separated from the local disturbances. It has the lowest magnetic intensities (7 722.7 nT) depicting the accumulation of sediments.

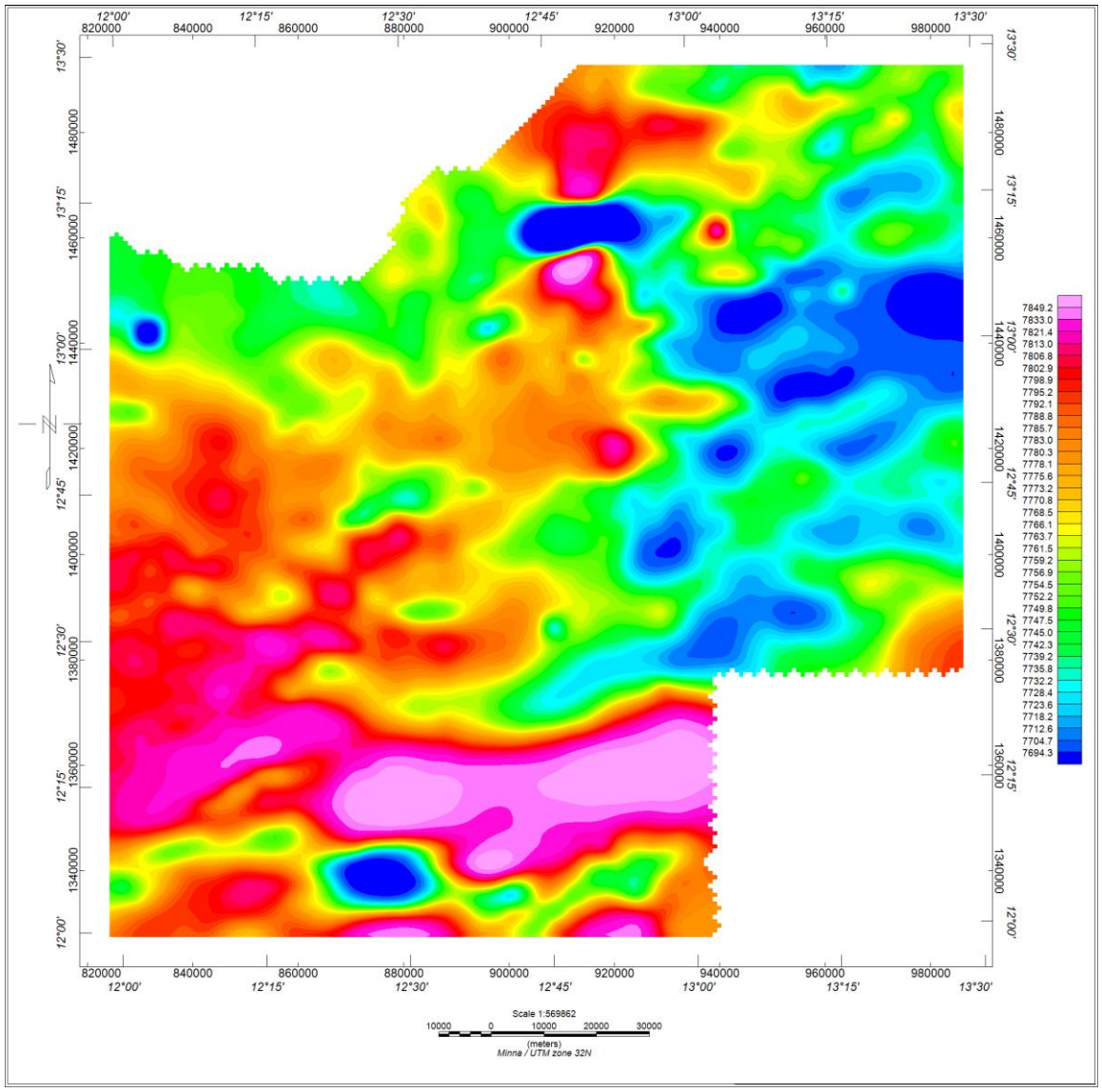

Figure 4.6: Upward Continuation (1 km) of the Total Magnetic Intensity Map of Parts of Borno Basin.

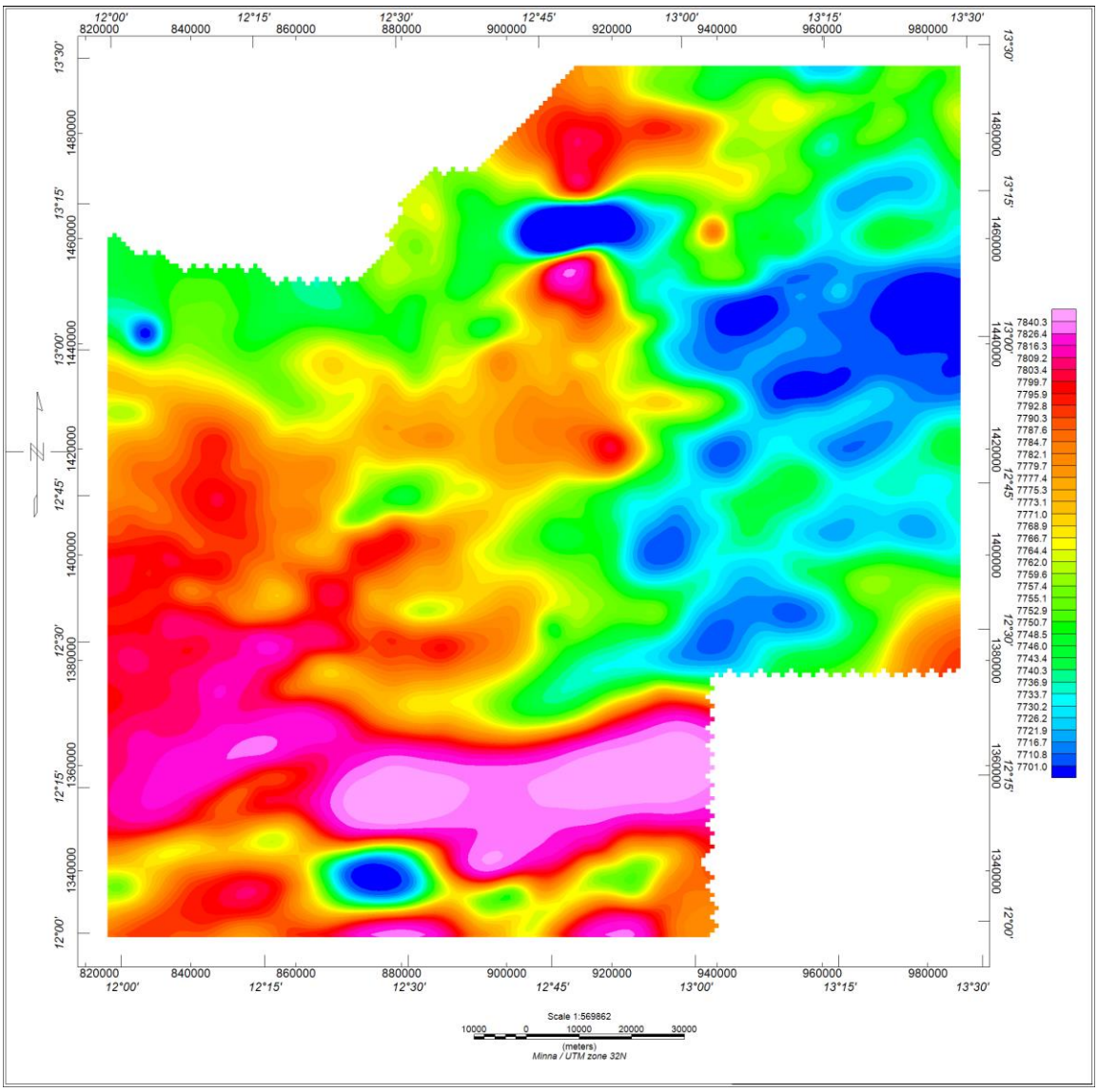

Figure 4.7: Upward Continuation (2 km) of the Total Magnetic Intensity Map of Parts of Borno Basin.

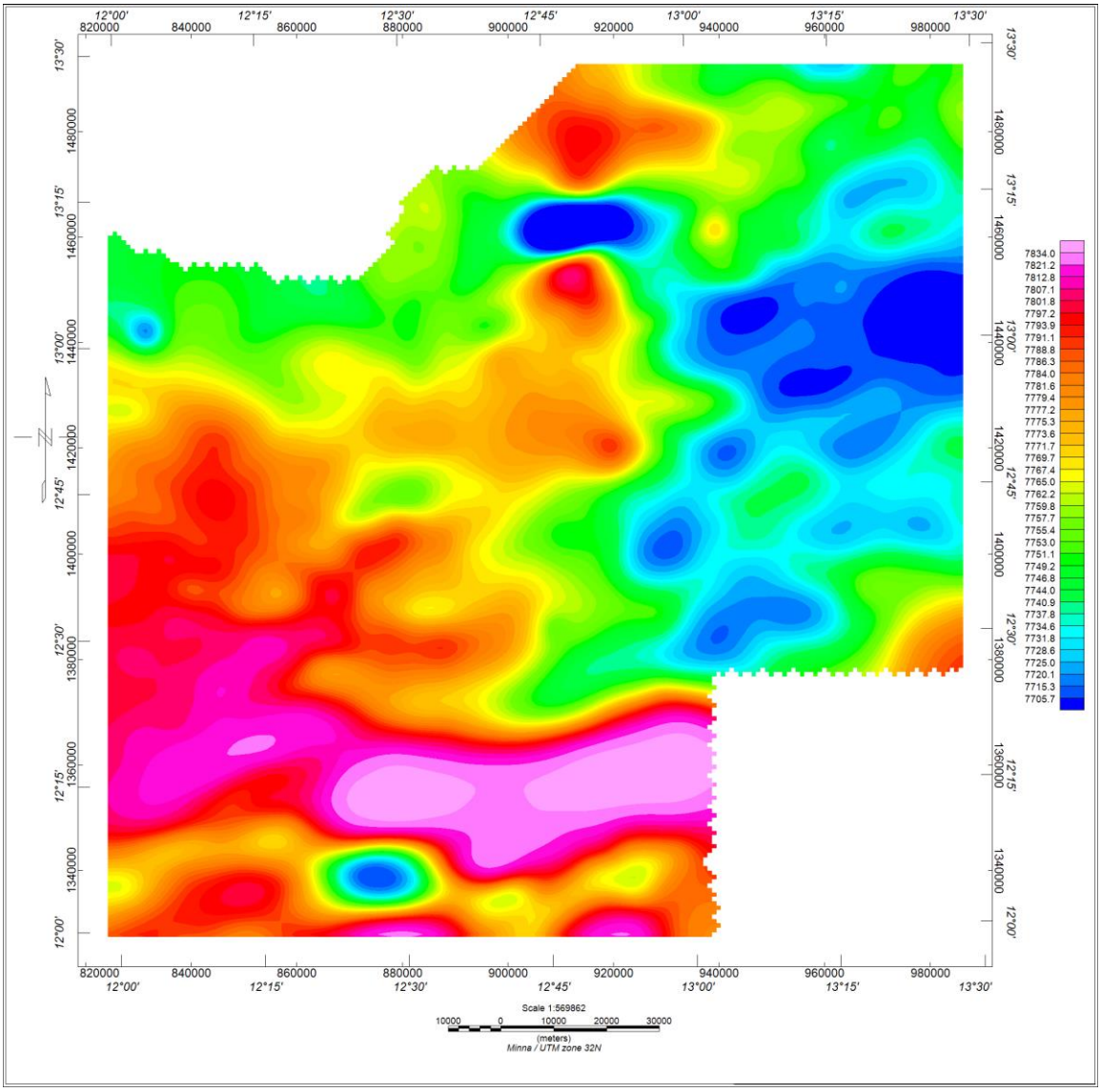

Figure 4.8: Upward Continuation (3 km) of the Total Magnetic Intensity Map of Parts of Borno Basin.

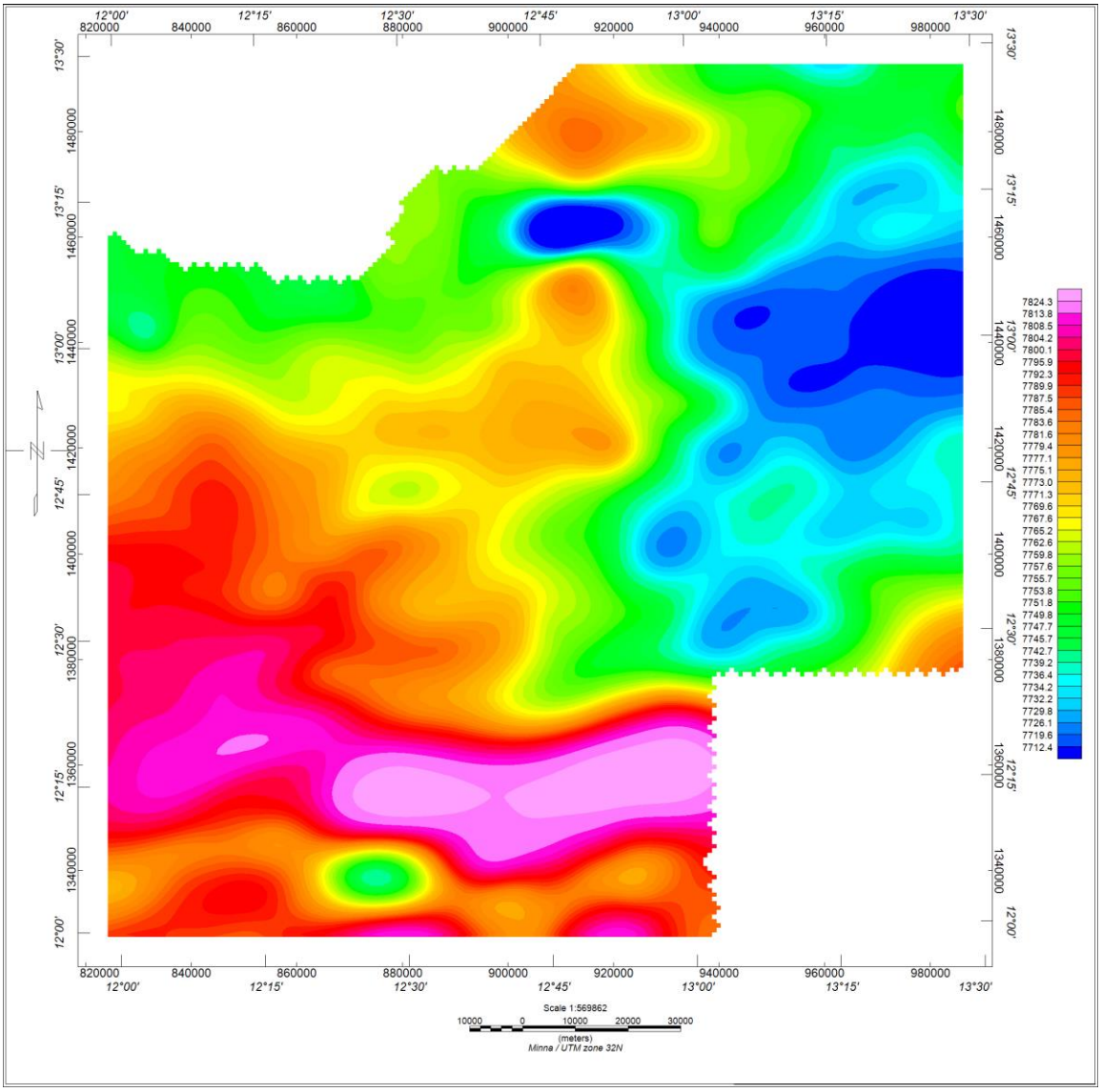

Figure 4.9: Upward Continuation (5 km) of the Total Magnetic Intensity Map of Parts of Borno Basin.

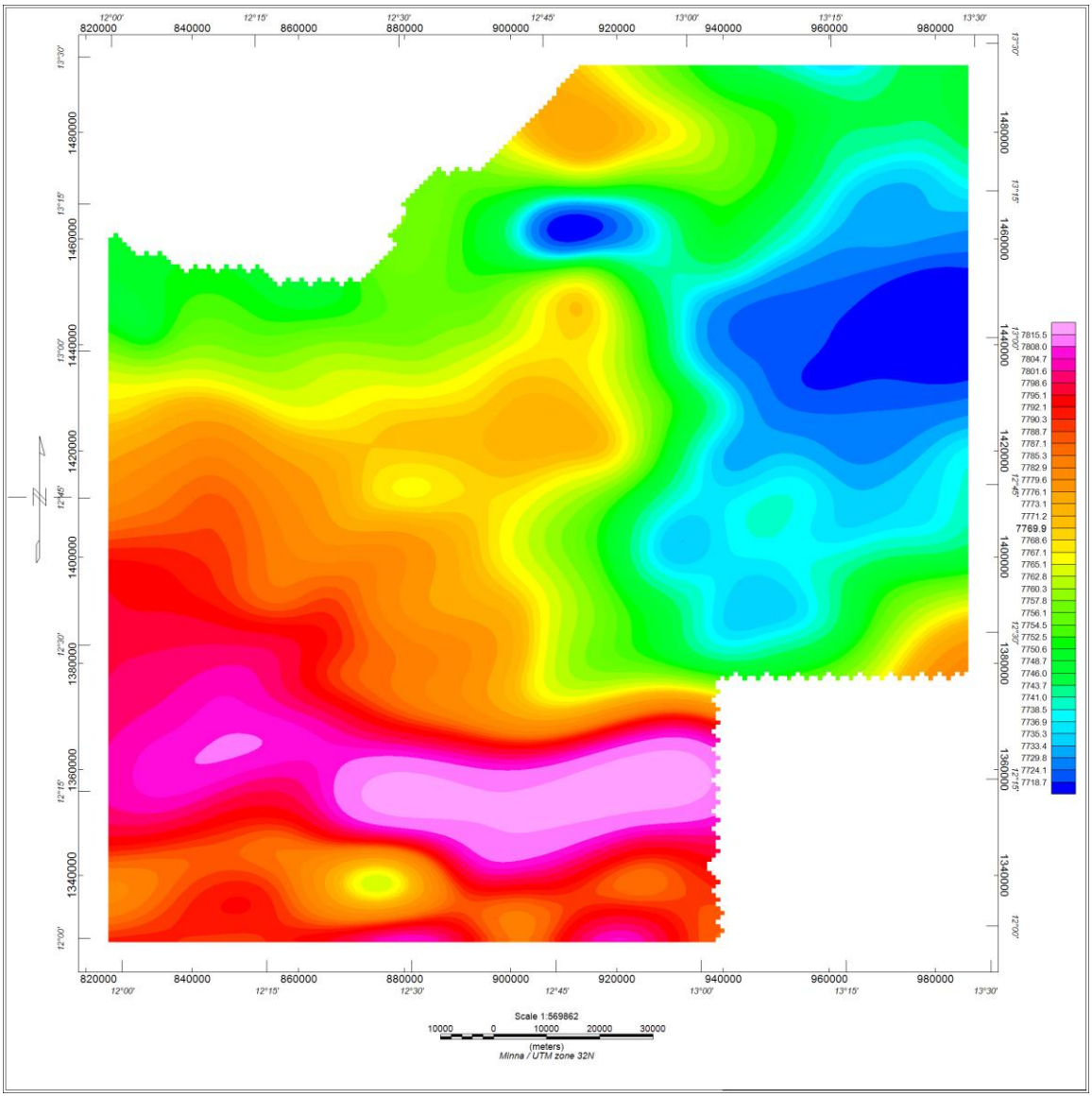

Figure 4.10: Upward Continuation (7.5 km) of the Total Magnetic Intensity Map of Parts of Borno Basin.

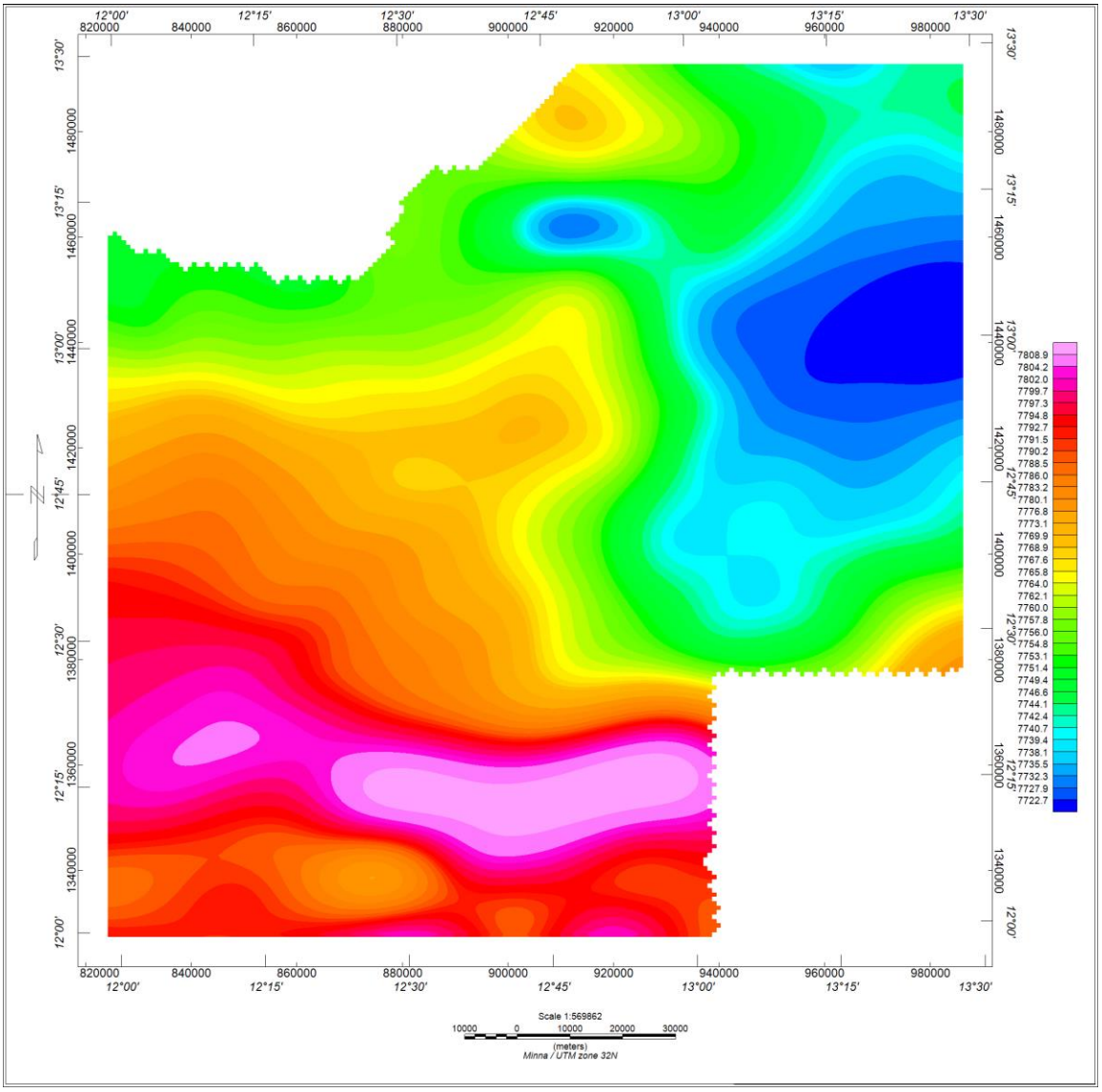

Figure 4.11: Upward Continuation (10 km) of the Total Magnetic Intensity Map of Parts of Borno Basin.

CHAPTER FIVE

5.0 CONCLUSION AND RECOMMENDATIONS

5.1 Conclusion

The result of the spectral analysis of the aeromagnetic data over parts of Borno Basin identified two main magnetic horizons under the area. The deeper sources are represented by the low frequency segments of the spectrum, while the shallower magnetic sources are represented by the high frequency segment of the spectrum.

The values of h_1 and h_2 obtained above were used to produce the contour maps of the first and second layers of spectral depth, Figures 4.2 and 4.4 and the surface plots equally for the first and second layers, Figures 4.3 and 4.5 were used for interpretations. The first layers, which are of shallower magnetic sources brought out by the above analysis, can be attributed mostly to lateritic ironstone capping and the effect of surrounding basement magnetic rocks. The second layer which is of deeper sources is equal to the thickness of the sediment basin. Other probable origin of the magnetic anomalies contributing to this layer is lateral variations in basement susceptibilities and intrabasement features like faults and fractures.

In either case, it can be reasonably deduced that the h_2 values obtained from the above spectral analysis represents the average depth of the basement complex in the section considered. These values of h_2 were used to obtain an approximate contour map of the basement surface in the basin as shown in Figure 4.4. Since the spectral depth evaluated represents the average depth at the centre of the section considered, the longitude and latitude values for the centre of each of the sixteen (16) sections were determined, from which the surface plot of the basement depth in the basin was generated.

A critical examination of Figure 4.4, second layer h_2 depth contour map, shows that the northeast of the study area around Karíriwa contains the highest accumulation of sediments (5.4 km). The Figure 4.11, upward continuation 10 km of the total magnetic intensity map of the study area, also shows that the same area has the lowest value of magnetic intensities (7 722.7 nT) depicting accumulation of sediments.

The two methods, spectral depth estimation and upward continuation analysis performed on the parts of Borno basin thus corroborate the finding that mineral deposits like hydrocarbon may be present.

5.2 Recommendations

The accumulation of sediments in the northeastern part of the Borno basin may suggests the presence of hydrocarbon. It is recommendable that more detailed seismic reflection survey be carried out in this area to corroborate the findings in this study.

REFERENCES

Ajakaiye, D.E. (1970). Gravity measurements over the Nigerian Younger granite province. *Earth Evolution Science*, 255, 50-52.

Ajakaiye, D.E. (1981). Geophysical investigation in the Benue trough: A review. *Earth Evolution Science*, 1, 110-125.

Ajakaiye, D.E., Hall, D.H., Ashiekaa J.A., & Udensi, E.E. (1991). Magnetic anomalies in the Nigerian continental mass based on aeromagnetic surveys. *Tectonophysics*, 192, 211-230.

Ajakaiye, D.E., Hall, D.H., & Millar, T.W. (1985). Interpretation of aeromagnetic data across the central crystalline shield areas of Nigeria. *Geophysical Journal Royal Astronomical Society London*, 83, 503-517.

Ajibade, A.C. (1976). Provisional classification and correlation of the schist belts in north-Western Nigeria. In C.A. Kogbe (Ed.), *Geology of Nigeria* (pp. 80-90). Nigeria, Ibadan: Elizabethan Publishing Company.

Ajibade, A.C. (1980). Geotectonic evolution of the Zungeru region Ph.D Thesis University College of Wales.

Ajibade, A.C., Woakes, M., & Rahaman, M.A. (1989). Proterozoic Crustal. In C.A. Kogbe (Ed.), *Geology of Nigeria* (pp. 57-69). Nigeria, Jos: Rock View Limited.

Ananaba, S.E., & Ajakaiye, D.E. (1987). Evidence of tectonic control of mineralization in Nigeria from lineament density analysis : A landsat study. *International Journal of Remote Sensing*, 8 (10), 1445-1453.

Avbovbo, A.A., Ayoola, E.O., & Osahon, G.A. (1986). Depositional and structural styles in Chad Basin of northeastern Nigeria. *Bulletin American Association Petroleum Geologists*, 70, 1787-1798.

Ball, E. (1980). An example of very consistent brittle deformation over a wide intercontinental area: The late Pan-African fracture system of the Taureg and Nigeria Shield. *Tectonic Physics*, 190, 211-230.

Barber, W. (1965). Pressure water in the Chad formation of Bomu and Dikwa emirates, northeastern Nigeria. *Bulletin Geological Survey Nigeria*, 35, 1-138.

Bath, M. (1974). *Spectral analysis in Geophysics*. Netherland, Amsterdam: Elsevier Publishing Company.

Bellion, Y.C. (1989). Histoire Geodynamique Post-Paleozoique de l'Afrique de l'ouest d'apres l'etude de quelques Bassins Sedimentaires (Senegal, Taoudenni, Iullemmeden, Tehad). *Publication Occasionnelle Centre International Formation Echanges Geologiques*, 17, 1- 302.

Benkhelil, J. (1988). Structure et Evolution Geodynamique du Bassin Intracontinental de la Benoue (Nigeria). *Bulletin Centres Recherches Exploration- Production Elf-Aquitaine*, 12, 29-128.

Benkhelil, J. (1989). The origin and evolution of the cretaceous Benue trough (Nigeria). *Journal African Earth Sciences*, 8, 251-282.

Black, R., Caby, R., Moussine-Pauchkie, A., Bayer, R., Bartrand J.M., Bovillier, A.M., Fabre, J., & Lesquer, A. (1979). Evidence for late precambrian plate tectonics in West Africa. Nature. *Tectonophysics*, 278, 223-227.

Carter, J.D., Barber, W., Tait, E.A., & Jones, G.P. (1963). The geology of parts of Adamawa, Bauchi and Bornu provinces in northeastern Nigeria. *Bulletin Geological Survey Nigeria*, 30, 1-99.

Cratchley C.R., & Jones, G.P. (1965). An interpretation of the geology and gravity anomalies of the Benue valley, Nigeria. *Overseas Geological Surveys Geophysical Paper*, 1, 1-26.

Cratchley, C.R., Louis, P., & Ajakaiye, D.E. (1984). Geophysical and geological evidence for the Benue-Chad basin cretaceous rift valley system and its tectonic implications. *Journal African Earth Sciences*, 2, 141-150.

Dessauvagie, T.F.J. (1974). Geological Map of Nigeria (scale 1:100,000): Nigeria Mining, Geological and Metallurgical Society, Ibadan, Nigeria.

Dessauvagie, T.F.J. (1975). Explanatory note to the Geological Map of Nigeria. *Journal of Mining and Geology*, 9, 3-28.

Dobrin, M.B. (1976). Introduction to Geophysical Prospecting (3rd ed.). New York, NY: McGraw Hill.

Eborall, A.C. (1976). Intermediate rocks from older granite complexes of the Bauchi area, northern Nigeria. In C.A. Kogbe (Ed.). *Geology of Nigeria Publication*, (pp. 65-74) Nigeria, Jos: Rock View Limited.

Fairhead, J.D. (1986). Geophysical controls on sedimentation within the African rift systems. *Spectral Publication Geological Society, London*, 25, 19-27.

Fairhead, J.D., & Okereke C.S. (1987). A regional gravity study of the West African rift system in Nigeria and Cameroon and its tectonic interpretation. *Tectonophysics*, 143, 1-3. (15), 141-159.

Fairhead, J.D., & Okereke C.S. (1988). Depths to major density contrasts beneath the West African rift system in Nigeria and Cameroon based on the spectral analysis of gravity data. *Journal of African Earth Sciences*, 7, (5-6), 769-777.

Fairhead, J.D., & Green, C.M. (1989). Controls on rifting in Africa and the regional tectonic model for the Nigeria and East Niger rift basins. *Journal of African Earth Sciences*, 8, (2-4), 231-249.

Falconer, J.D. (1911). The geology and geography of northern Nigeria. London, UK: MacMillan.

Ford, S.O. (1981). The economic mineral resources of the Benue trough. *Earth Evolution Sciences* , 1, (2), 154-163.

Genik, G.J. (1993). Petroleum geology of the cretaceous-tertiary rift basins in Niger, Chad and the Central African Republic. *Bulletin American Association Petroleum Geologists*, 77, 1405-1434.

Geological Survey of Nigeria. (1956). *Nigeria and the Cameroons*: *Lexique Stratigraphique* (4th ed.). France, Paris : Furon, R.

Geological Survey of Nigeria. (1974). Geological Map of Nigeria. Scale 1:2,000,000: Geological Survey of Nigeria, Kaduna, Nigeria.

Grant, F.S., & West, G.F. (1965). Interpretation theory in Applied Geophysics. New York, NY: McGraw- Hill Book Company.

Grant, N.K. (1978). Structural distinction between a sedimentary cover and an underlying basement in the 600Myrs old Pan-African domain of northern Nigeria. *Geology Society of America Bulletin*, 89, 50-58.

Guiraud, M. Binks, R.M., Fairhead, J.D., & Wilson, M. (1992). Chronology and geodynamic setting of cretaceous-cenozoic rifting in West and Central Africa. *Tectonophysics*, 213, 227-234.

Guiraud, M., Ajakaiye, D.E., & Ugodulunwa, F.X.O. (1989). Characterization of late Cretaceous NE-SW sinistral wrench faults in the Upper Benue Trough (Nigeria) using micro-tectonic and aeromagnetic data. *Journal of African Earth Sciences*, 9, (1), 9-21.

Hahn, A., Kind E.G., & Mishra, D.C (1976): Depth Estimate of magnetic Sources by means of Fourier amplitude spectra. *Geophysical Prospecting*, 24, 287-308.

Johnson, W.W. (1969). A Least-Squares Method of Interpreting Magnetic Anomalies caused by Two-Dimensional Structures. *Geophysics*, 34, 65 – 74.

Jones, B. (1932). The Geology of Southern Borno: Annual Report Geological Survey Nigeria. *Geology Survey of Nigeria Bulletin*, 31, 9-14.

Jones, H.A., & Hockney, R.D. (1964). The Geology of parts of southwestern Nigeria. *Geology Survey of Nigeria Bulletin*, 31, 1-130.

Kearey, P., Brooks, M., & Hill, I. (2002). An Introduction to Geophysical Exploration (3rd ed.). United Kingdom, UK: Blackwell Publishing Company.

Keller, G.R., Wendlandt, R.F., & Bott, M.H.P. (1995). West and Central African Rift System. In K. H. Olsen (Ed.), *Continental Rifts* (pp. 437-449). Netherland, Amsterdam: Elsevier Publishing Company.

King, L.C. (1950). Speculations on the outline and the mode of disruption of Gondwanaland. Geological Magazine, 87, 353-359.

Likkasson, O.K., Ajayi, C.O., & Shemang, E.M. (2005). Some structural features of the middle Benue trough, Nigeria, modeled from aeromagnetic anomaly Data. Science Forum: *Journal of Pure and Applied Science*, 8, 100-125.

Lochner, J., Mattson, B., Gibb, M., & Newman, P. (2010, February 3). Spectral Analysis. Spectral Analysis of the Residual Field, 1, 1. Retrieved from imagine.gsfc.nasa.gov/docs/science/how_I1/spectral.html. 10 May, 2012.

Matheis, G. (1976). Short review of the geology of the Chad basin in Nigeria. In C.A. Kogbe (pp. 289-294). Nigeria, Lagos: Elizabethan Publishing Company.

McCurry, P. (1976). The geology of the precambrian to lower paleiozoic rocks of northern Nigeria-a Review. In C.A. Kogbe (Ed.), *Geology of Nigeria* (pp. 15-39). Nigeria, Lagos: Elizabethan Publishing Company.

Miller, R.E., Johnston, R.H., Oluwa, J.A.I., & Uzoma, J.U. (1968). Groundwater Hydrology of the Chad Basin in Bornu and Dikra Emirates, Northern Nigeria with special emphasis on the Flow life of the Artesian System. Water Supply Paper United States Geological Survey 1957-1, 1-148.

Obi, G.C. (1995). Stratigraphic Succession and Age of Cretaceous Sedimentary Rocks in the Hawal Basin, NE Nigeria. *Journal Mining and Geology*, 30, 195-203.

Obi, G.C. (1998). Upper Cretaceous Gongila Formation in the Hawal Basin, Northeast Benue Trough: A Storm and Wave Dominated Regressive Shoreline Complex. *Journal African Earth Sciences*, 26, 619-632.

Okosun, E.A. (1992). Cretaceous Ostracod Biostratigraphy from Chad Basin in Nigeria. *Journal African Earth Sciences*, 14, 327-339.

Okosun, E.A. (1995). Review of the Geology of Bornu Basin. *Journal of Mining and Geology*, 31, 113-122.

Olugbemiro, O.R. (1997). Hydrocarbon Potential, Maturation and Palaeoenvironments of the Cretaceous (Cenomanian-Santonian) Series in the Bornu (Chad) Basin, NE Nigeria. *Journal of Mining and Geology*, 14, 150.

Oyawoye, M.O. (1964). The Geology of the Nigeria basement complex. *Journal of Mining Geology And Metallurgical Society*, 1, 87-102.

Pal, P.C., Khurana, K.K., & Unikdishman, P. (1978). Two examples of Spectral approach to source depth estimation in gravity and magnetic pageoph, 177, 772 – 783.

Raeburn, C., & Jones, B. (1934). The Chad Basin: Geology and Water Supply. *Bulletin Geological Survey Nigeria*, 15, 1-61.

Reeves, C. (2005). Aeromagnetic Surveys: Principles, Practice and Interpretation. *Bulletin Geological Survey of Nigeria*, 20, 55-56.

Reyment, R.A. (1965). *Aspects of the Geology of Nigeria*. Nigeria, Ibadan: Ibadan University Press.

Russ, W. (1957): The Geology of Parts of Niger, Zaria and Sokoto Provinces, with Special Reference to the Occurrence of Gold. *Bulletin Geological Survey Nigeria*, 27, 1-42.

Sahagian, D.L. (1993). Structural Evolution of African Basins: Stratigraphic Synthesis. *Basin Research*, 5, 41-54.

Spector, A., & Grant, F.S. (1970). Statistical models for interpreting aeromagnetic data. *Geophysics*, 35, 293-302.

Spectral Analysis (Waveform and Fourier Analysis). Retrieved from artisites.ucsc.edu/ems/music/tech_background/TE-04/teces_04.html. 10 May, 2012.

Skeels, D.C. (1967). What is Residual Gravity? *Geophysics*, 32, 872 -876.

Stuart, G.W., Fairhead, J.D., Dorbath, L., & Dorbath, C. (1985). A Seismic Refraction Study of the Crustal Structure Associated with the Adamawa Plateau and Garoua Rift, Cameroun, West Africa. *Geophysical Journal Royal Astronomical Society London*, 81, 1- 12.

Telford, W.M.N., Geldart, L.P., Sheriff, R.E., & Keys, D.A. (1976). *Applied Geophysics*. Cambridge: Cambridge University Press.

Truswell, F.B., & Cope, R.N. (1963). The geology of parts of Nigeria and Zaria provinces, northwestern Nigeria. *Bulletin Geology Society of Nigeria*, 29,53-55.

Udensi, E.E. (2001). Interpretation of the total magnetic field over the Nupe basin in West Central Nigeria using aeromagnetic data. Ph.D thesis ABU, Zaria, Nigeria.

Whiteman, A.J. (1982). *Nigeria: Its Petroleum Geology, Resources and potential*. London, UK : Graham and Trotman Press.

Wright, J.B. (1968). South Atlantic continental Drift and the Benue Trough. *Tectonophysics*, 64, 301-310.

Wright, J.B., Hastings, D.A., Jones, W.B., & Williams, H.R. (1995). Geology and Mineral Resources of West Africa. *Journal of Mining Geology and Geological Society*, 15, 90-120.

Zaborski, P.M., Ugodulunwa, F., Idornigie, A., Nnabo, P., & Ibe K. (1998). Stratigraphy and Structure of the Cretaceous Gongola basin, Northeast Nigeria. *Bulletin Centres Recherches Exploration-Production Elf-Aquitaine* ,21, 153-185.

APPENDIX A

SPECTRAL ENERGIES AND THEIR CORRESPONDING WAVE NUMBERS FOR SIXTEEN OVERLAPPING BLOCKS/CELL DIVISIONS WITH X AND Y COORDINATES REPRESENTING FREQUENCY AND LOGARITHM RESPECTIVELY.

Spectral 1

S/no	X	Y
	Freq (rads/km)	Log (en)
1	0.126	19.508
2	0.252	19.200
3	0.377	19.575
4	0.503	18.442
5	0.629	17.547
6	0.755	17.715
7	0.881	16.948
8	1.006	16.726
9	1.132	16.539
10	1.258	16.296
11	1.384	16.819
12	1.509	16.926
13	1.635	16.727
14	1.761	16.999
15	1.887	16.584
16	2.013	16.476
17	2.138	16.477
18	2.264	16.606
19	2.390	16.237
20	2.516	16.328
21	2.642	16.175
22	2.767	16.242

Spectral 2

S/no	X	Y
	Freq (rads/km)	Log (en)
1	0.126	21.166
2	0.252	21.286
3	0.377	20.587
4	0.503	19.353
5	0.629	18.996
6	0.755	19.426
7	0.881	18.913
8	1.006	18.688
9	1.132	18.329
10	1.258	18.100
11	1.384	18.015
12	1.509	18.139
13	1.635	17.898
14	1.761	17.511
15	1.887	17.922
16	2.013	17.916
17	2.138	18.140
18	2.264	17.616
19	2.390	17.439
20	2.516	18.060
21	2.642	18.020
22	2.767	17.932

Spectral 3

S/no	X	Y
	Freq (rads/km)	Log (en)
1	0.126	20.480
2	0.252	19.106
3	0.377	19.167
4	0.503	18.068
5	0.629	17.172
6	0.755	17.252
7	0.881	16.727
8	1.006	17.039
9	1.132	16.588
10	1.258	16.426
11	1.384	16.317
12	1.509	16.447
13	1.635	16.497
14	1.761	16.656
15	1.887	16.599
16	2.013	16.337
17	2.138	16.803
18	2.264	16.641
19	2.390	16.635
20	2.516	16.757
21	2.642	16.562
22	2.767	16.464

Spectral 4

S/no	X	Y
	Freq (rads/km)	Log (en)
1	0.126	21.941
2	0.252	20.401
3	0.377	19.476
4	0.503	18.896
5	0.629	18.114
6	0.755	18.607
7	0.881	18.452
8	1.006	18.098
9	1.132	18.166
10	1.258	17.755
11	1.384	17.705
12	1.509	17.737
13	1.635	18.080
14	1.761	17.950
15	1.887	17.989
16	2.013	17.745
17	2.138	17.810
18	2.264	17.748
19	2.390	17.814
20	2.516	18.130
21	2.642	17.897
22	2.767	17.856

Spectral 5

S/no	X	Y
	Freq (rads/km)	Log (en)
1	0.126	21.391
2	0.252	20.822
3	0.377	18.585
4	0.503	17.366
5	0.629	18.173
6	0.755	17.699
7	0.881	17.471
8	1.006	17.498
9	1.132	17.586
10	1.258	17.508
11	1.384	17.249
12	1.509	17.141
13	1.635	17.361
14	1.761	17.904
15	1.887	17.402
16	2.013	17.190
17	2.138	17.738
18	2.264	17.288
19	2.390	17.054
20	2.516	17.221
21	2.642	17.123
22	2.767	17.029

Spectral 6

S/no	X	Y
	Freq (rads/km)	Log (en)
1	0.126	19.911
2	0.252	18.457
3	0.377	18.519
4	0.503	17.696
5	0.629	16.853
6	0.755	16.902
7	0.881	16.373
8	1.006	15.833
9	1.132	16.154
10	1.258	15.924
11	1.384	15.805
12	1.509	15.997
13	1.635	15.963
14	1.761	16.224
15	1.887	16.111
16	2.013	15.735
17	2.138	16.348
18	2.264	15.798
19	2.390	15.709
20	2.516	15.785
21	2.642	15.799
22	2.767	15.468

Spectral 7

S/no	X	Y
	Freq (rads/km)	Log (en)
1	0.126	20.739
2	0.252	19.702
3	0.377	18.140
4	0.503	17.790
5	0.629	17.061
6	0.755	16.659
7	0.881	16.876
8	1.006	17.610
9	1.132	17.450
10	1.258	16.751
11	1.384	17.546
12	1.509	17.923
13	1.635	17.598
14	1.761	17.764
15	1.887	18.033
16	2.013	17.528
17	2.138	17.868
18	2.264	17.654
19	2.390	17.703
20	2.516	17.695
21	2.642	17.729
22	2.767	17.706

Spectral 8

S/no	X	Y
	Freq (rads/km)	Log (en)
1	0.126	21.138
2	0.252	18.792
3	0.377	19.149
4	0.503	18.334
5	0.629	16.902
6	0.755	17.840
7	0.881	17.104
8	1.006	17.136
9	1.132	17.038
10	1.258	16.421
11	1.384	17.383
12	1.509	17.427
13	1.635	17.388
14	1.761	17.226
15	1.887	17.164
16	2.013	17.259
17	2.138	17.180
18	2.264	17.021
19	2.390	17.123
20	2.516	17.159
21	2.642	16.906
22	2.767	16.886

Spectral 9

S/no	X	Y
	Freq (rads/km)	Log (en)
1	0.126	20.882
2	0.252	18.865
3	0.377	19.668
4	0.503	18.249
5	0.629	17.116
6	0.755	17.611
7	0.881	16.805
8	1.006	16.666
9	1.132	16.734
10	1.258	16.308
11	1.384	16.410
12	1.509	16.376
13	1.635	16.458
14	1.761	16.296
15	1.887	16.374
16	2.013	16.451
17	2.138	16.417
18	2.264	16.290
19	2.390	16.040
20	2.516	16.082
21	2.642	15.889
22	2.767	15.935

Spectral 10

S/no	X	Y
	Freq (rads/km)	Log (en)
1	0.126	19.461
2	0.252	17.808
3	0.377	17.732
4	0.503	16.339
5	0.629	15.874
6	0.755	16.263
7	0.881	15.701
8	1.006	15.481
9	1.132	15.464
10	1.258	14.615
11	1.384	15.723
12	1.509	15.698
13	1.635	15.691
14	1.761	15.242
15	1.887	15.369
16	2.013	15.860
17	2.138	16.118
18	2.264	15.645
19	2.390	15.573
20	2.516	15.931
21	2.642	15.814
22	2.767	15.748

Spectral 11

S/no	X	Y
	Freq (rads/km)	Log (en)
1	0.126	19.461
2	0.252	17.808
3	0.377	17.732
4	0.503	16.339
5	0.629	15.874
6	0.755	16.263
7	0.881	15.701
8	1.006	15.481
9	1.132	15.464
10	1.258	14.615
11	1.384	15.723
12	1.509	15.698
13	1.635	15.691
14	1.761	15.252
15	1.887	15.369
16	2.013	15.860
17	2.138	16.118
18	2.264	15.635
19	2.390	15.573
20	2.516	15.931
21	2.642	15.814
22	2.767	15.748

Spectral 12

S/no	X	Y
	Freq (rads/km)	Log (en)
1	0.126	20.076
2	0.252	18.394
3	0.377	17.777
4	0.503	16.340
5	0.629	16.267
6	0.755	16.439
7	0.881	16.040
8	1.006	15.965
9	1.132	15.958
10	1.258	15.100
11	1.384	15.766
12	1.509	15.965
13	1.635	15.888
14	1.761	15.476
15	2.887	15.513
16	2.013	15.523
17	2.138	15.391
18	2.264	15.202
19	2.390	15.088
20	2.516	14.983
21	2.642	14.773
22	2.767	14.845

Spectral 13

S/no	X	Y
	Freq (rads/km)	Log (en)
1	0.126	19.394
2	0.252	17.204
3	0.377	17.344
4	0.503	16.813
5	0.629	15.513
6	0.755	15.700
7	0.881	15.439
8	1.006	15.831
9	1.132	15.744
10	1.258	15.249
11	1.384	15.906
12	1.509	15.903
13	1.635	15.830
14	1.761	15.852
15	1.887	15.582
16	2.013	15.283
17	2.138	15.641
18	2.264	15.588
19	2.390	15.528
20	2.516	15.309
21	2.642	15.282
22	2.767	15.374

Spectral 14

S/no	X	Y
	Freq (rads/km)	Log (en)
1	0.126	18.985
2	0.252	17.666
3	0.377	16.826
4	0.503	16.187
5	0.629	16.181
6	0.755	15.411
7	0.881	15.040
8	1.006	15.340
9	1.132	15.238
10	1.258	14.697
11	1.384	15.262
12	1.509	15.367
13	1.635	14.908
14	1.761	15.230
15	1.887	14.956
16	2.013	14.612
17	2.138	14.780
18	2.264	14.622
19	2.390	14.648
20	2.516	14.489
21	2.642	14.461
22	2.767	14.394

Spectral 15

S/no	X	Y
	Freq (rads/km)	Log (en)
1	0.126	20.318
2	0.252	17.680
3	0.377	18.696
4	0.503	17.262
5	0.629	16.380
6	0.755	16.873
7	0.881	16.475
8	1.006	16.574
9	1.132	16.518
10	1.258	16.031
11	1.384	16.548
12	1.509	16.835
13	1.635	16.727
14	1.761	16.777
15	1.887	16.448
16	2.013	16.325
17	2.138	16.655
18	2.264	16.582
19	2.390	16.525
20	2.516	16.520
21	2.642	16.382
22	2.767	16.387

Spectral 16

S/no	X	Y
	Freq (rads/km)	Log (en)
1	0.126	21.002
2	0.252	19.019
3	0.377	19.842
4	0.503	18.807
5	0.629	17.489
6	0.755	18.454
7	0.881	17.709
8	1.006	17.760
9	1.132	17.334
10	1.258	17.240
11	1.384	17.762
12	1.509	17.590
13	1.635	17.483
14	1.761	17.561
15	1.887	17.414
16	2.013	17.236
17	2.138	17.290
18	2.264	17.198
19	2.390	17.329
20	2.516	17.333
21	2.642	17.086
22	2.767	17.096

APPENDIX B

GRAPHICAL PLOT OF LOGARITHM OF SPECTRAL ENERGIES AGAINST THEIR CORRESPONDING WAVE- NUMBERS FOR SIXTEEN OVERLAPPING SECTIONS BLOCKS/CELL DIVISIONS.

Section 1

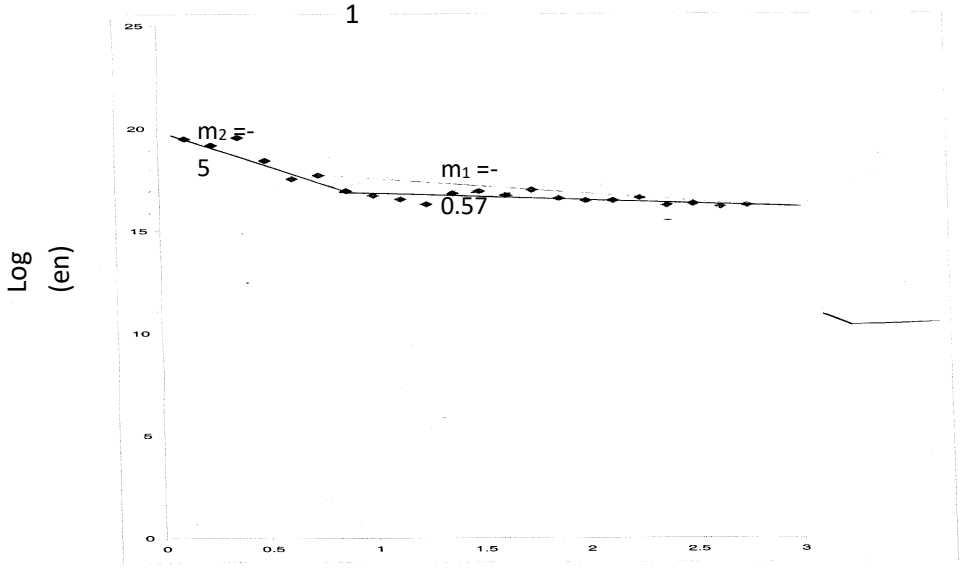

Section 2

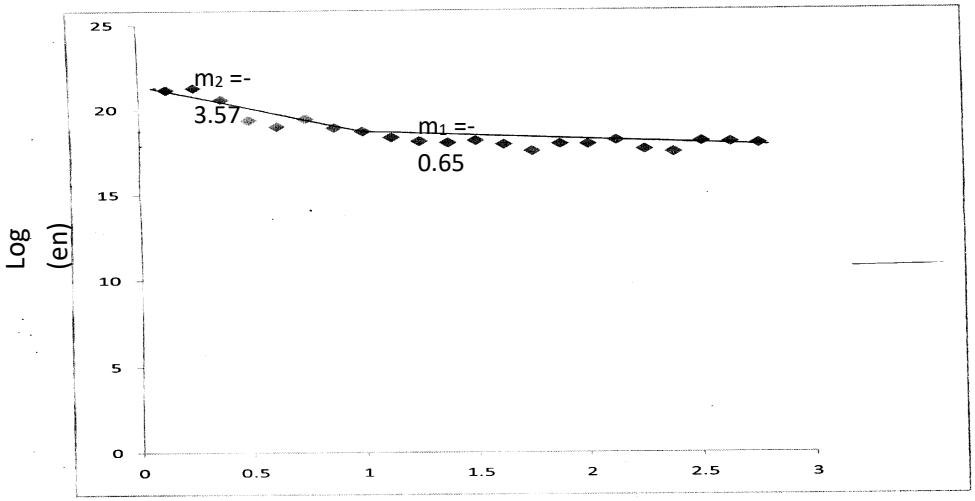

Figure A.1: Energy Spectra of Sections 1 and 2 with Gradient of first and second Linear Segment as m_1 and m_2 respectively.

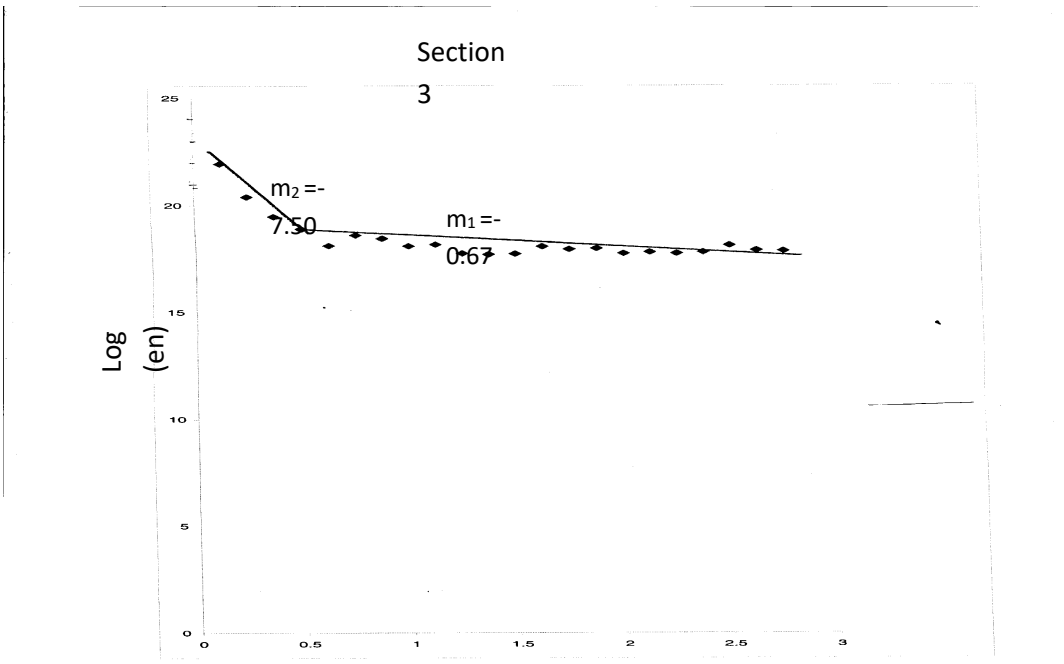

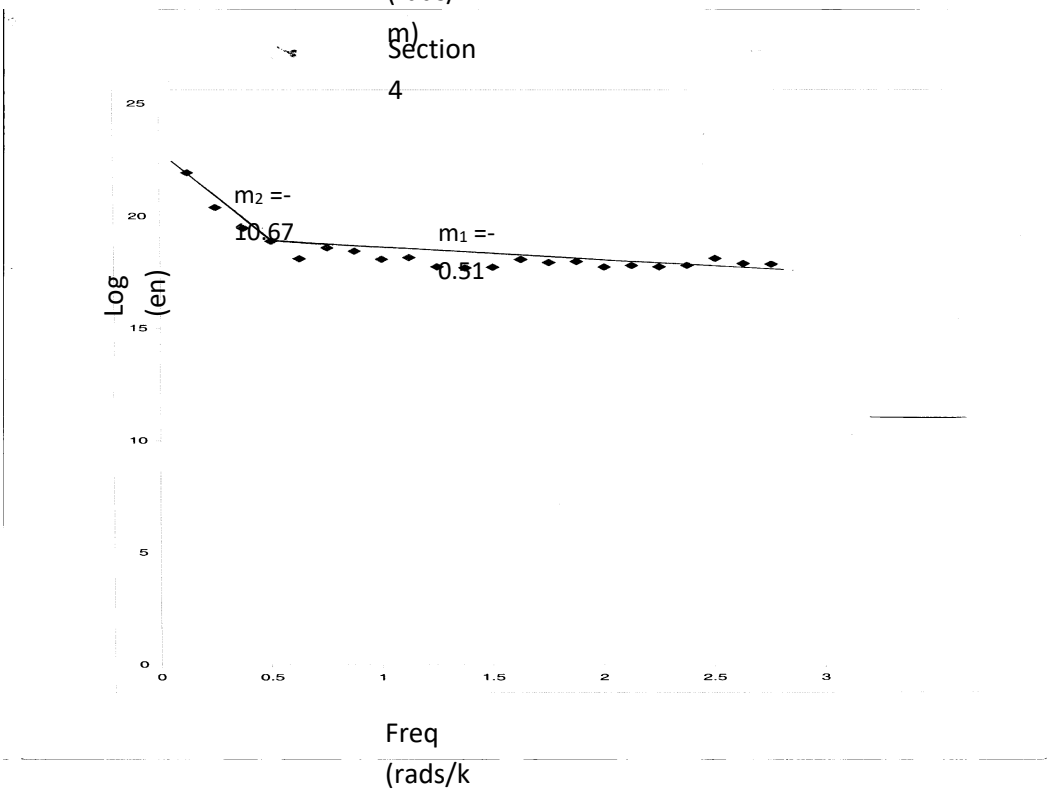

Figure A.2: Energy Spectra of Sections 3 and 4 with Gradient of first and second Linear Segment as m_1 and m_2 respectively.

Secti
on 5

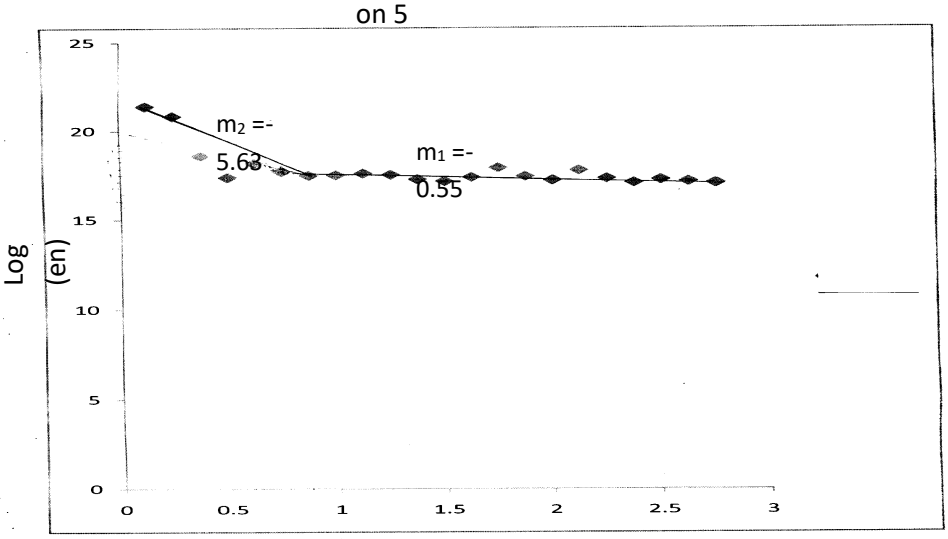

Freq
(rads/k
m)

Section
6

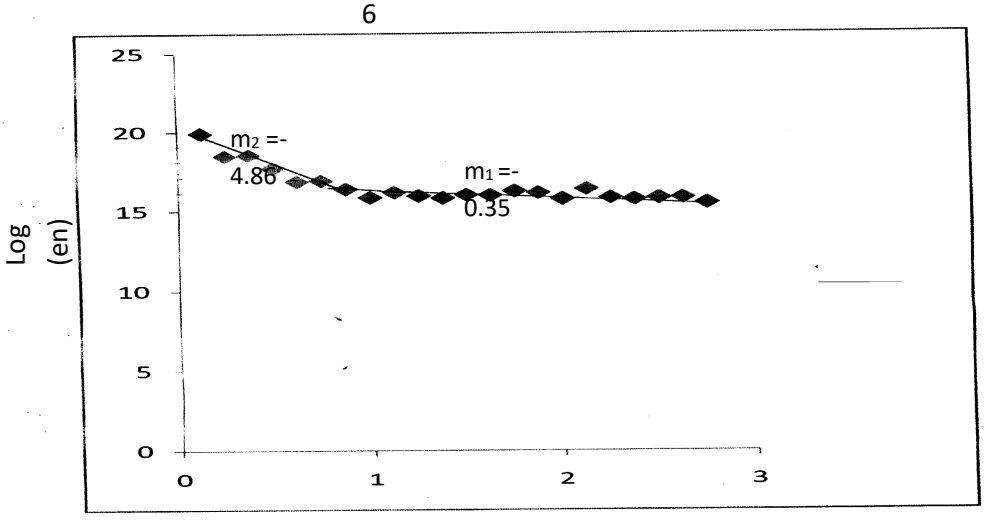

Freq
(rads/k
m)

Figure A.3: Energy Spectra of Sections 5 and 6 with Gradient of first and second Linear Segment as m_1 and m_2 respectively.

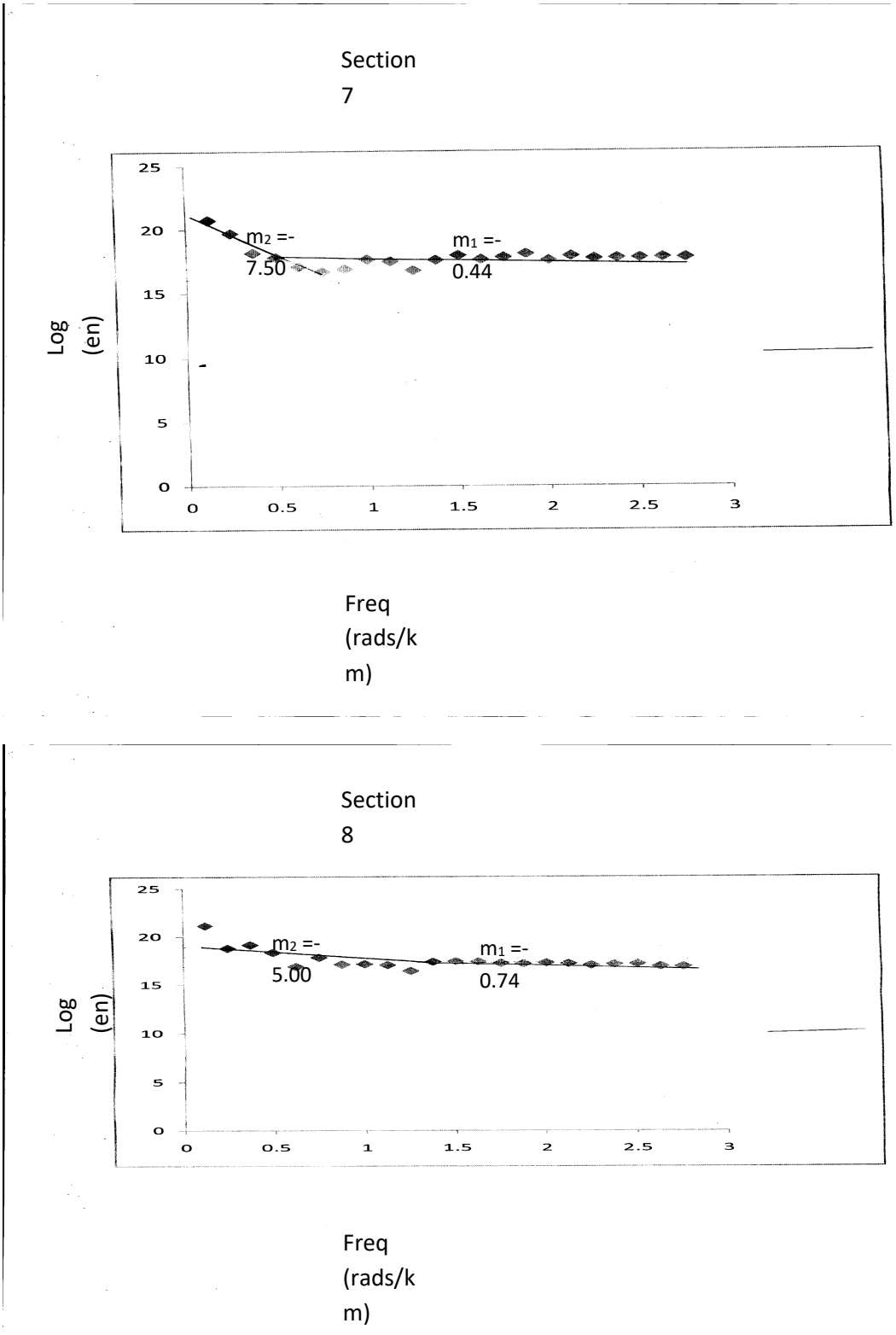

Figure A.4: Energy Spectra of Sections 7 and 8 with Gradient of first and second Linear Segment as m_1 and m_2 respectively.

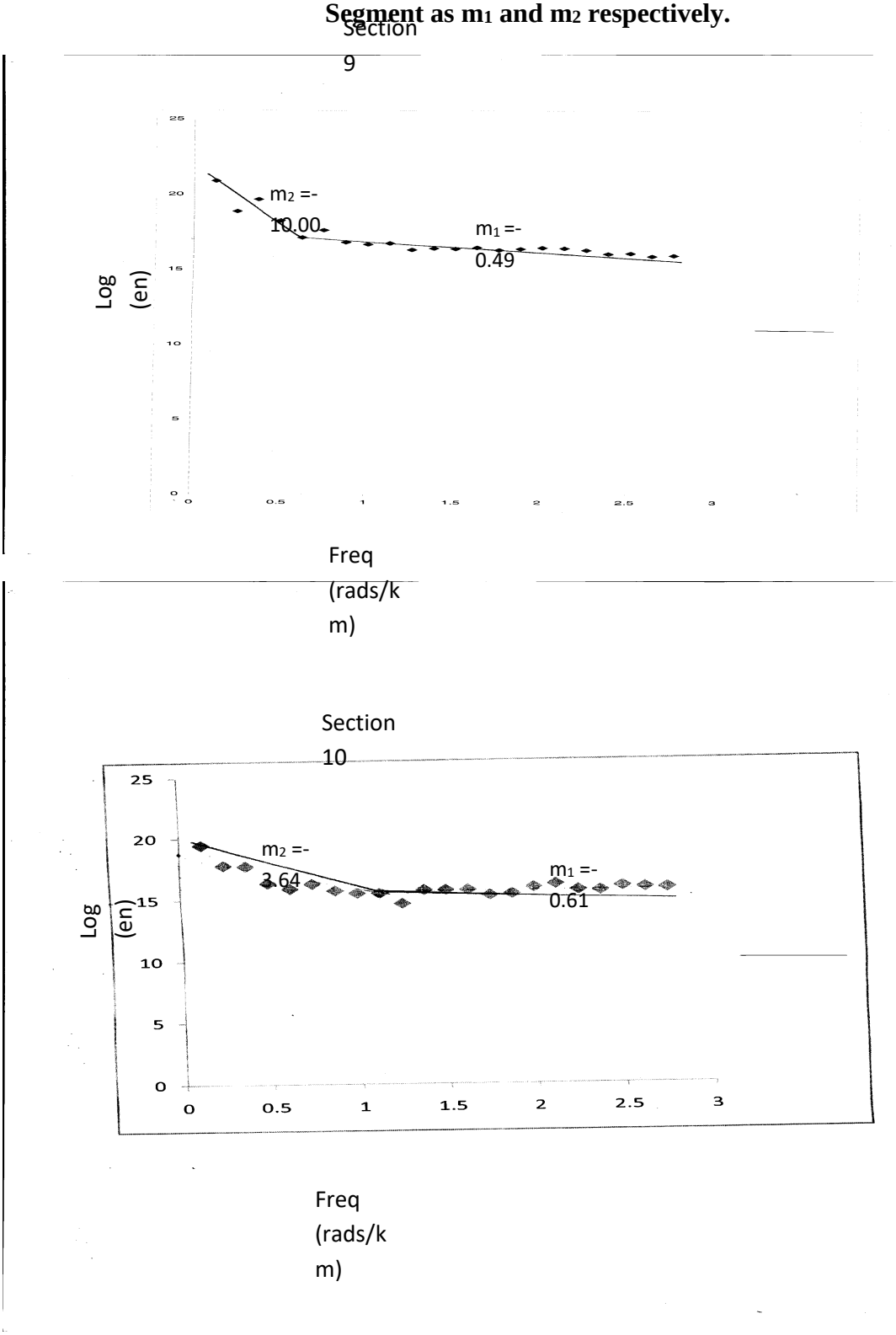

Figure A.5: Energy Spectra of Sections 9 and 10 with Gradient of first and second Linear Segment as m_1 and m_2 respectively.

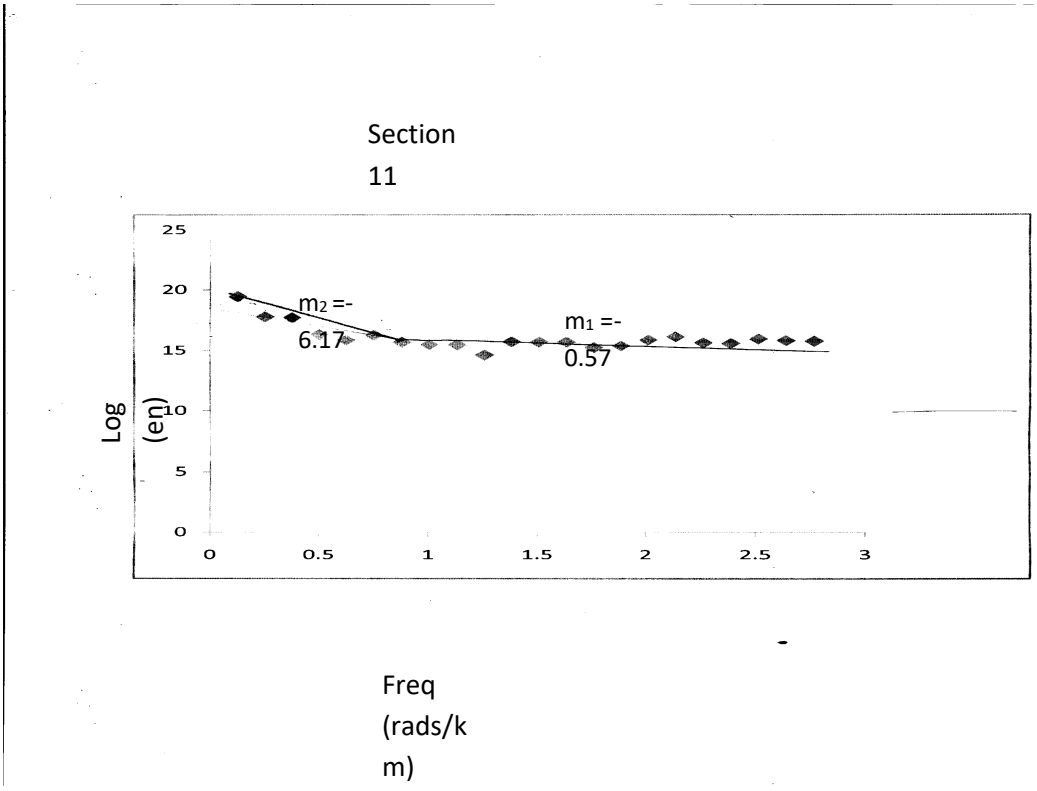

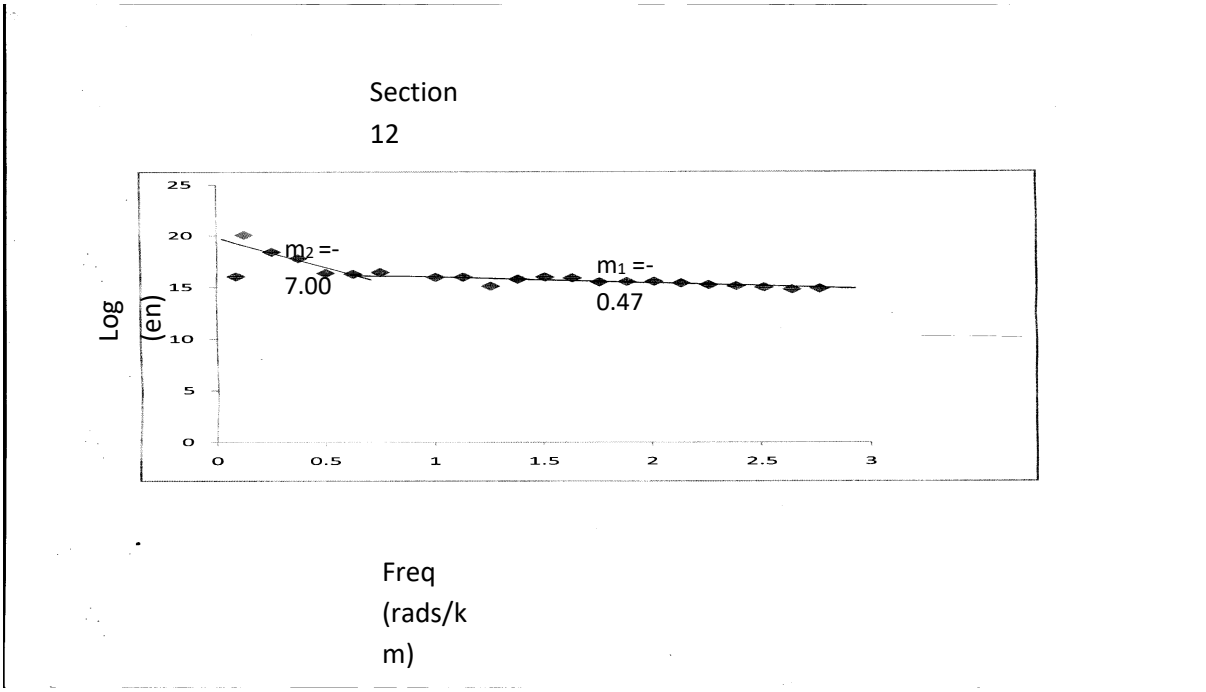

Figure A.6: Energy Spectra of Sections 11 and 12 with Gradient of first and second Linear Segment as m_1 and m_2 respectively.

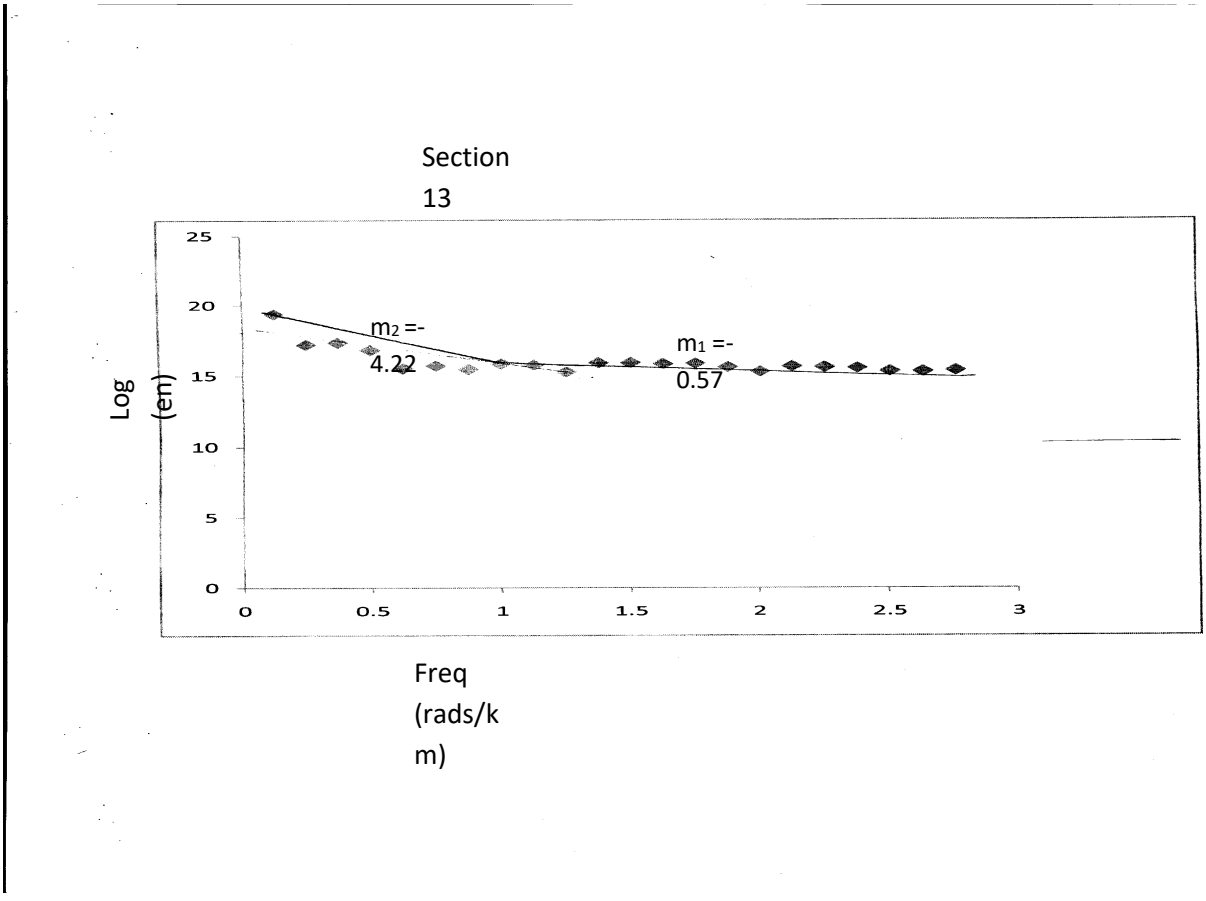

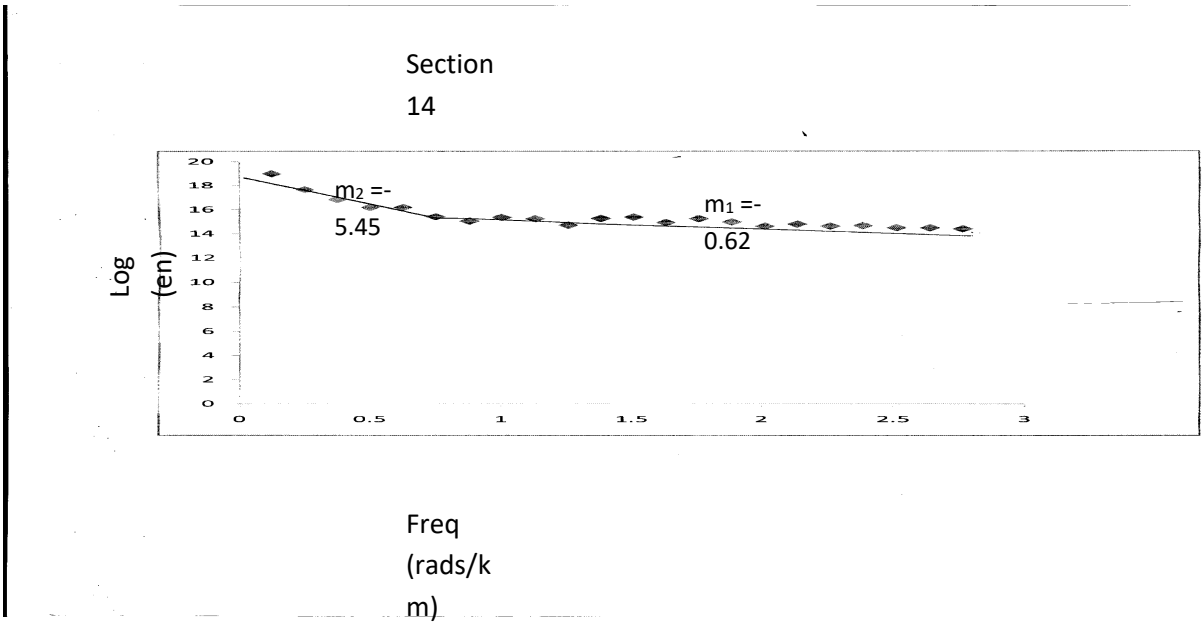

Figure A.7: Energy Spectra of Sections 13 and 14 with Gradient of first and second Linear Segment as m_1 and m_2 respectively.

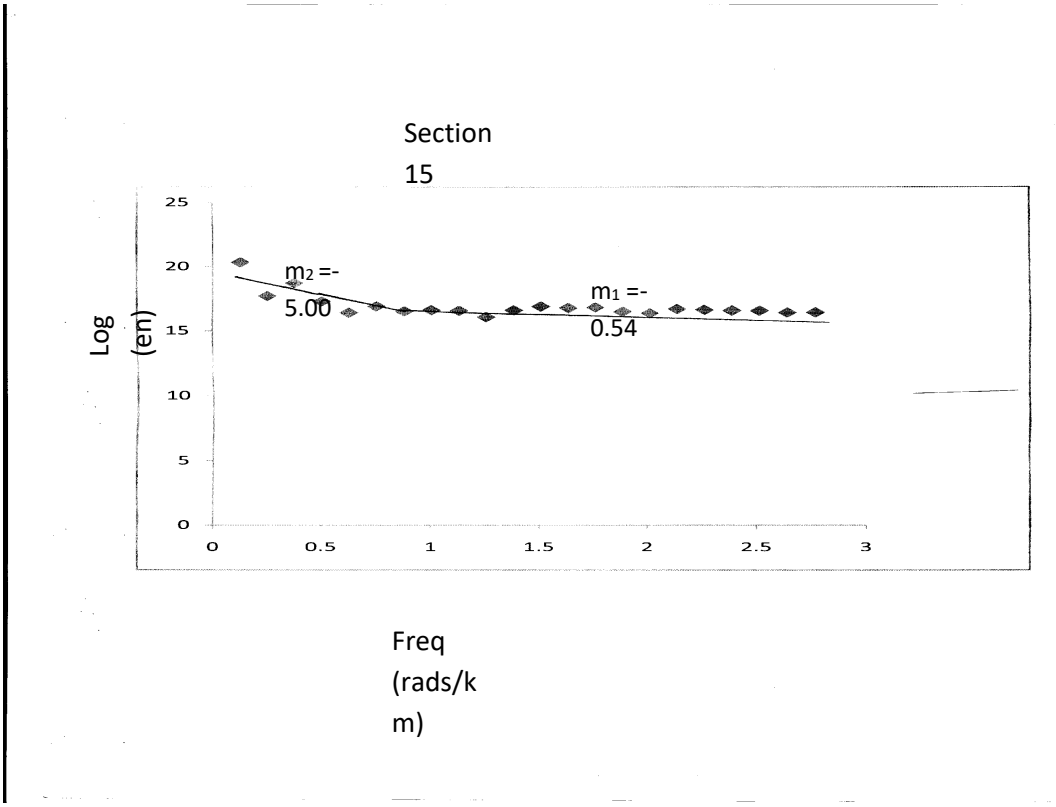

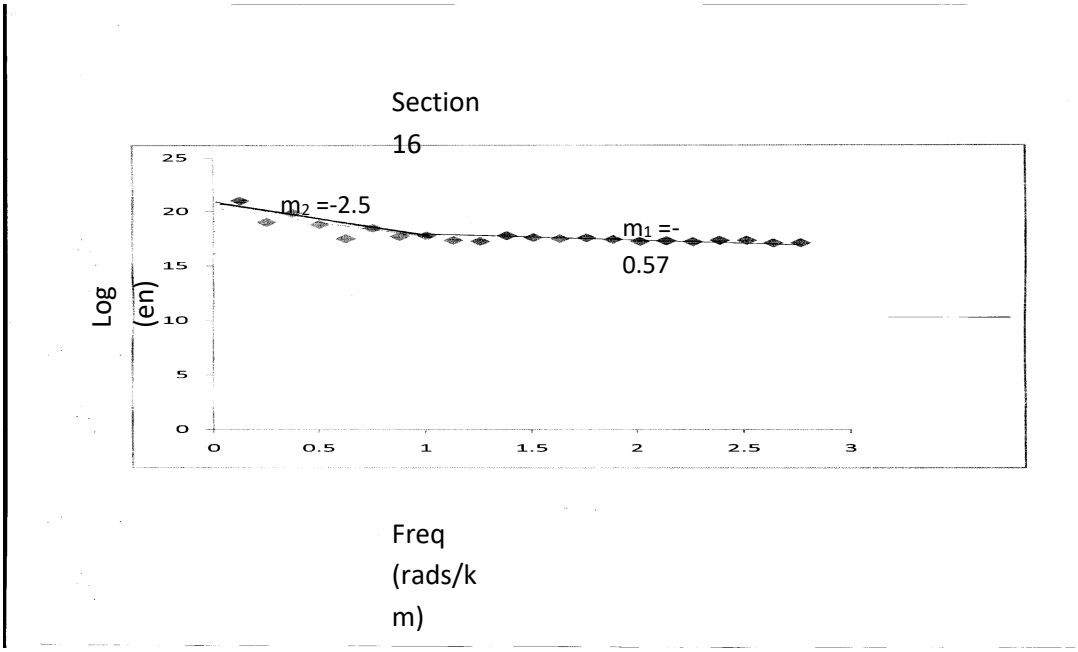

Figure A.8: Energy Spectra of Sections 15 and 16 with Gradient of first and second Linear Segment as m_1 and m_2 respectively.